Intense highly charged heavy ion beam production

T. NAKAGAWA (RIKEN)

1.Introduction

2.Ion sources for pulsed beam production(physics and technology)
- 2-1. Electron beam ion source
- 2-2. Laser ion source

3.Ion sources for DC beam production(physics and technology)
- 3-1. Electron cyclotron resonance ion source

Heavy ion accelerator facilities in the world

BNL RHIC

GSI

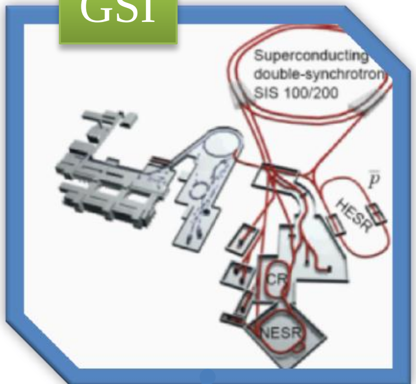

HIRFL(Lanzhou)

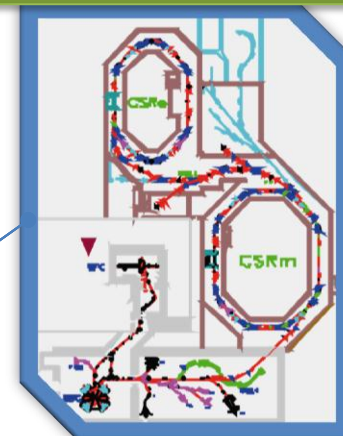

FRIB (MSU)

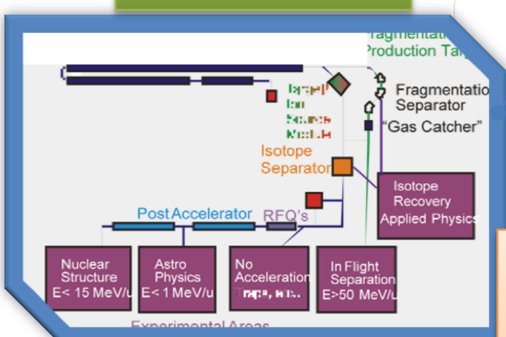

RIKEN RIBF

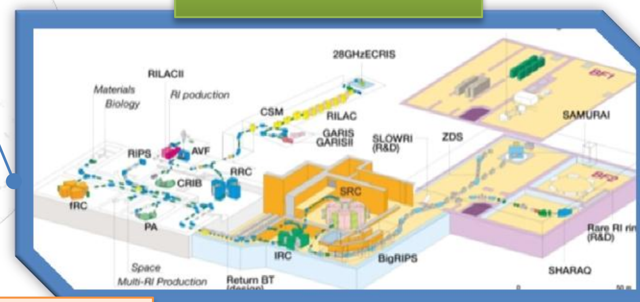

Intense beam of highly charged heavy ions

Au^{32+} 2.7x109/pulse

$U^{33+,34+}$ 8pμA

Ar^{12+} 1mA……………

Production rate of RI

Production rate of Radio isotope

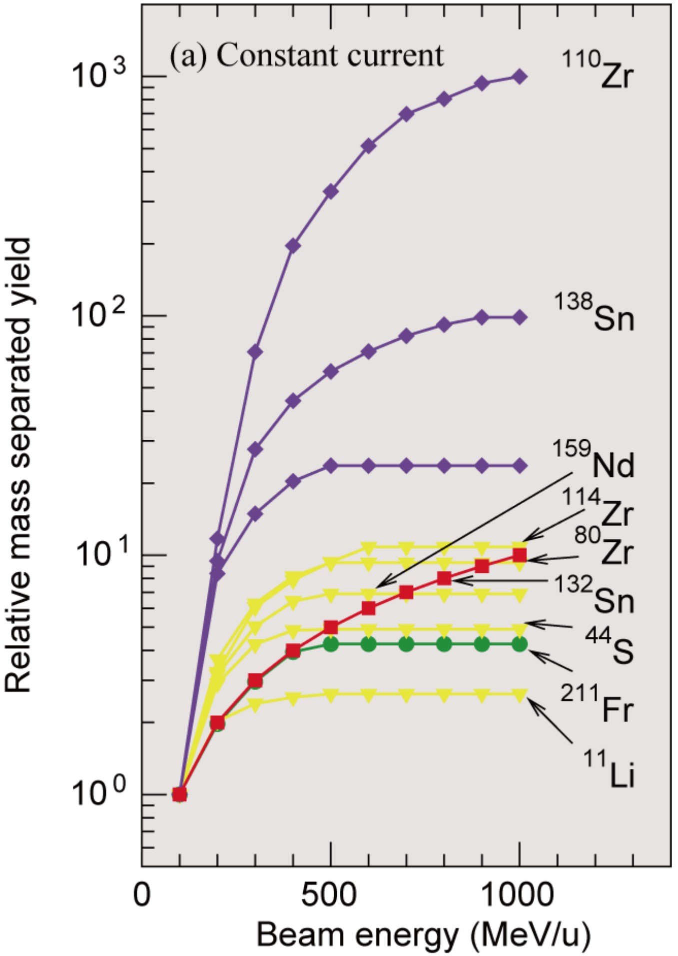

C. Jiang et al, NIM A492(2002)57

Production rate of Radio isotope

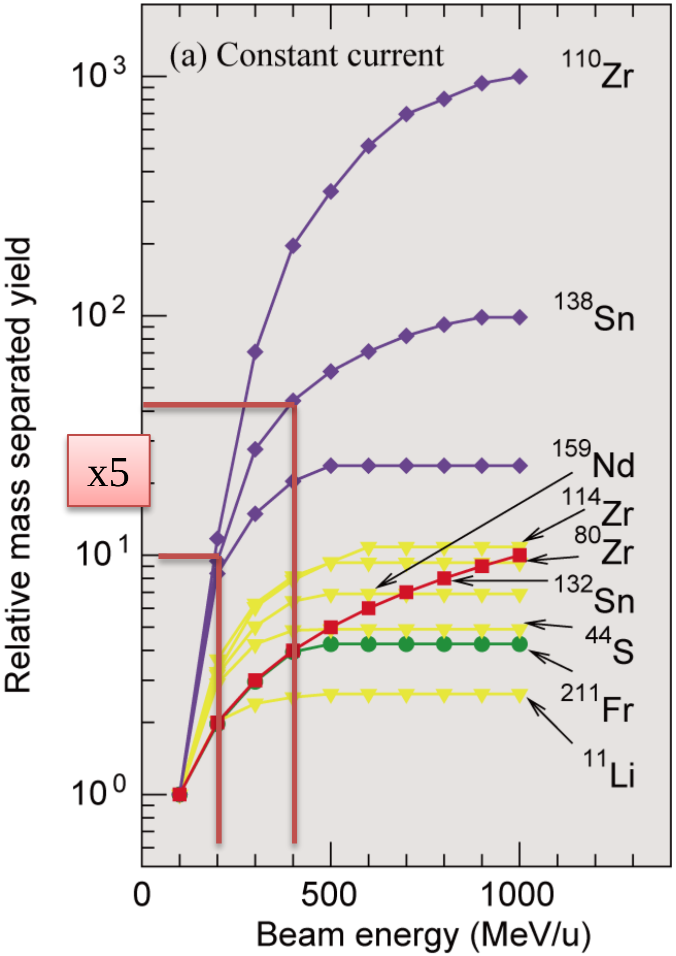

C. Jiang et al, NIM A492(2002)57

★In the case of ^{138}Sn production by an in-flight uranium fission reaction, we obtain only ~5 times the production gain by increasing the energy from 200 MeV/u to 400 MeV/u.

Production rate of RI

Production rate of Radio isotope

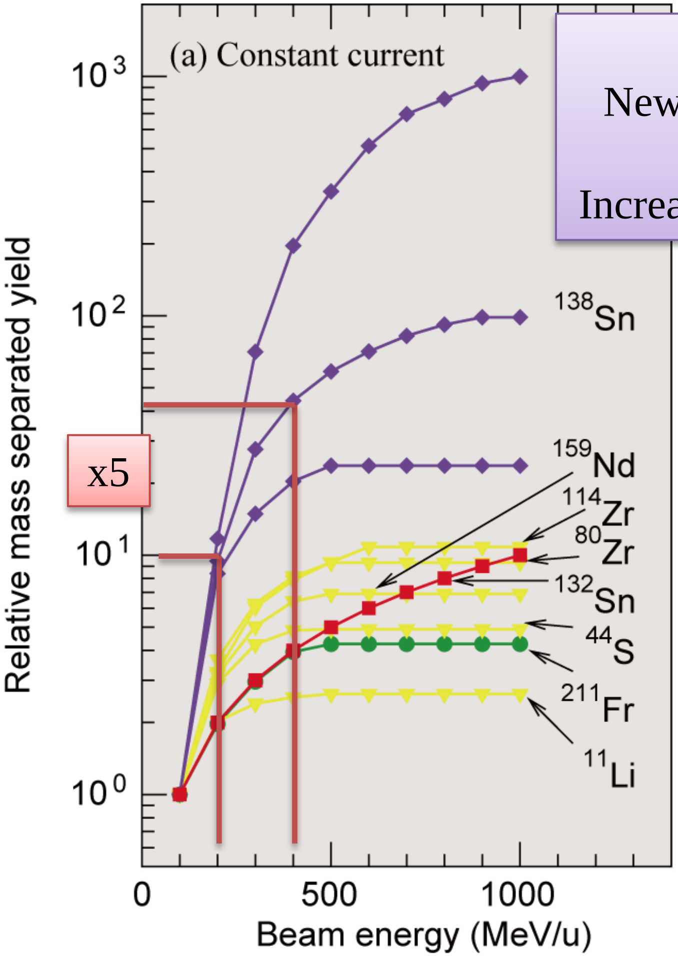

Construction cost
New ECRIS << New accelerator

Increase of RI beam(factor of five)

★In the case of ^{138}Sn production by an in-flight uranium fission reaction, we obtain only ~5 times the production gain by increasing the energy from 200 MeV/u to 400 MeV/u.

★Construction cost of a new ECRIS that can increase the beam intensity by a factor of five is significantly less than the construction cost of additional accelerators required to increase the energy.

C. Jiang et al, NIM A492(2002)57

Production rate of RI

Production rate of Radio isotope

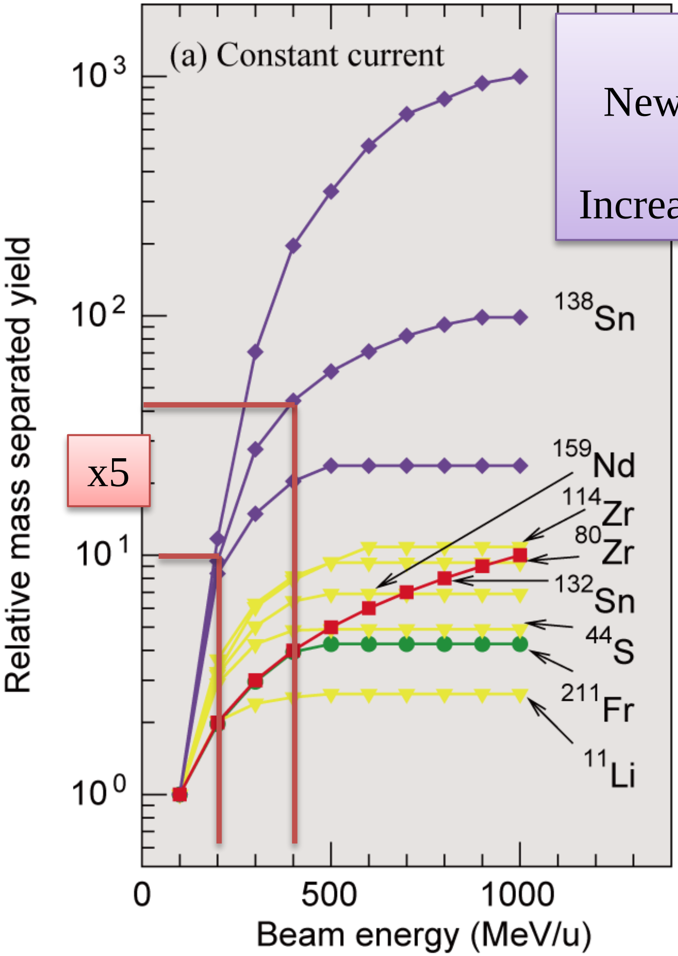

C. Jiang et al, NIM A492(2002)57

Construction cost
New ECRIS << New accelerator

Increase of RI beam(factor of five)

Time evolution of U beam

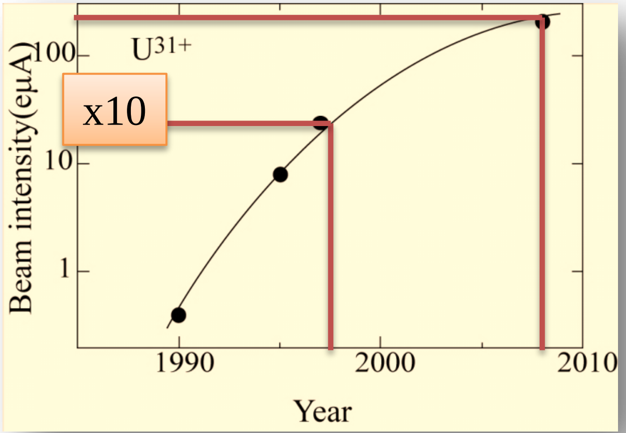

★In the case of ^{138}Sn production by an in-flight uranium fission reaction, we obtain only ~5 times the production gain by increasing the energy from 200 MeV/u to 400 MeV/u.

★Construction cost of a new ECRIS that can increase the beam intensity by a factor of five is significantly less than the construction cost of additional accelerators required to increase the energy.

★ In the past decade, the beam intensity of medium charge state of U ions, which is a suitable charge state for RIBF facility, has been increased by one order of magnitude.

Ion sources for Pulsed beam production

2.1 Electron beam ion sources (EBISs)

(I)Physics

(II)BNL-EBIS

(III)Beam instabilities

(IV)New developments

Tandem EBIS

The electron string ion source (ESIS)

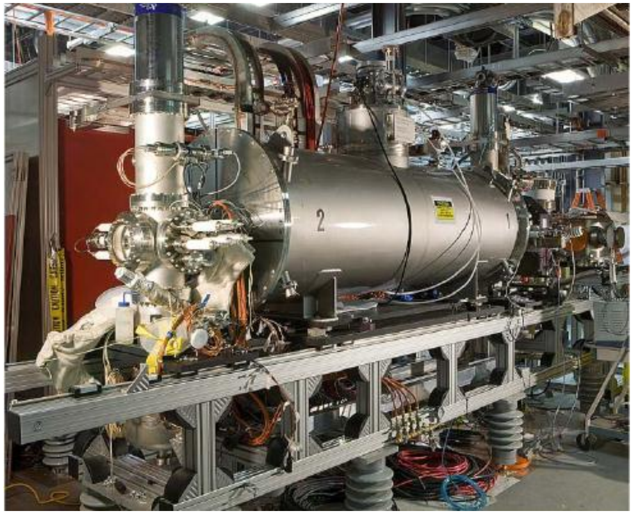

Electron Beam Ion Source (EBIS)-physics-

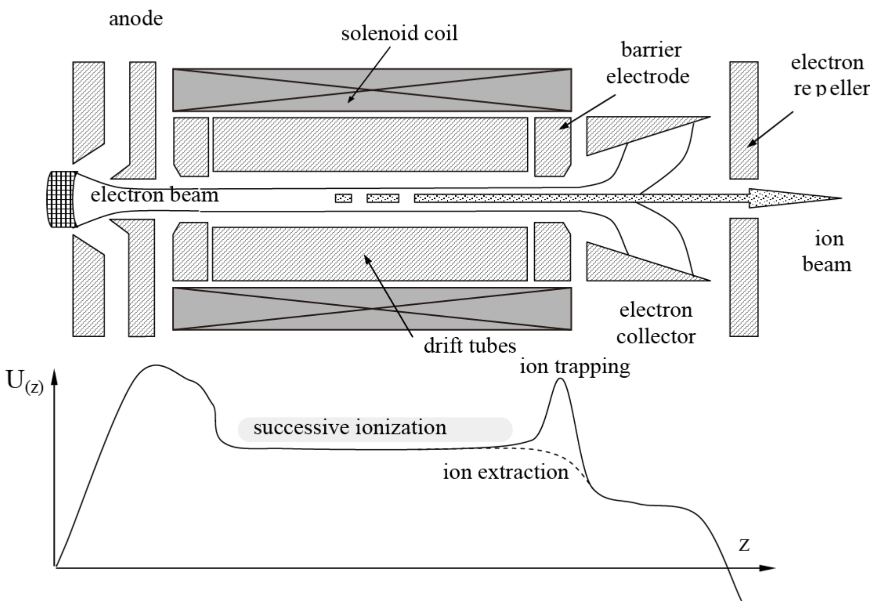

$$C^{+} = 3.36\times 10^{11} I_e L E_e$$

I_e : electron beam current
L : trap length
E_e: electron energy

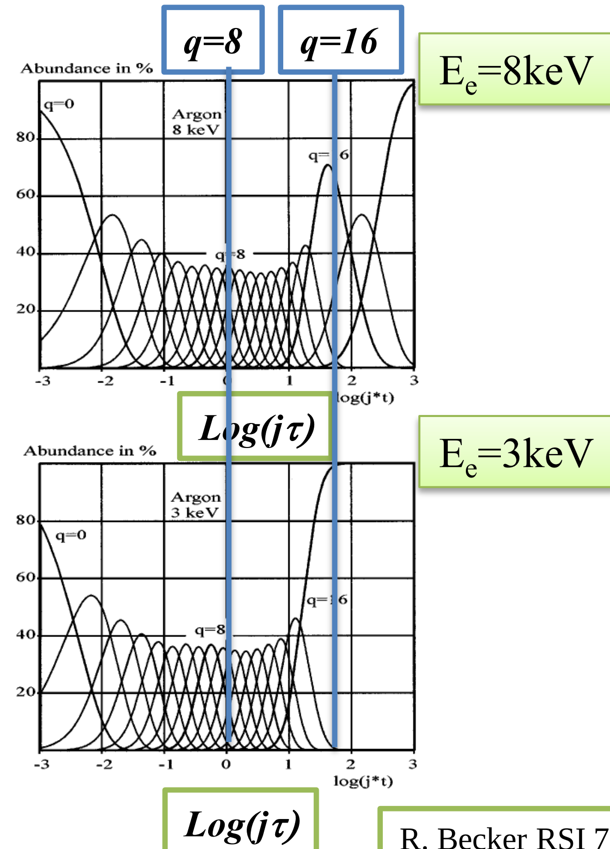

The EBIS has very unique feature that the total extracted charge per pulse is almost independent of ion species or charge state. Additionally, the beam pulse width can be controlled by the extraction barrier voltage manipulation, and therefore the both short pulses (~10μs) of high current (several mA) are possible. It is suited for single turn synchrotron injection.

R. Becker RSI 71(2000)816

EBIS for BNL RHIC

Requirements for pre-injector

Ion species	He~U
Beam intensity	He^{2+} $5x10^{10}$/pulse Fe^{20+} $4x10^{9}$ Au^{32+} $2.7x10^{9}$
Repetition rate	5Hz
Pulse width	10~40μs
Switching time	1 sec
Output energy	2MeV/amu

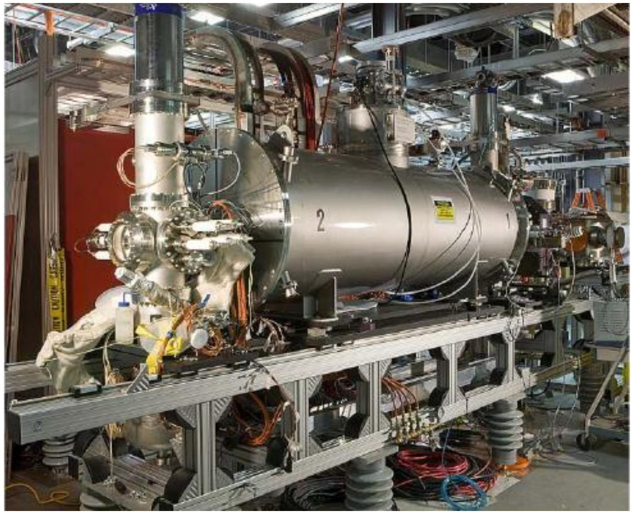

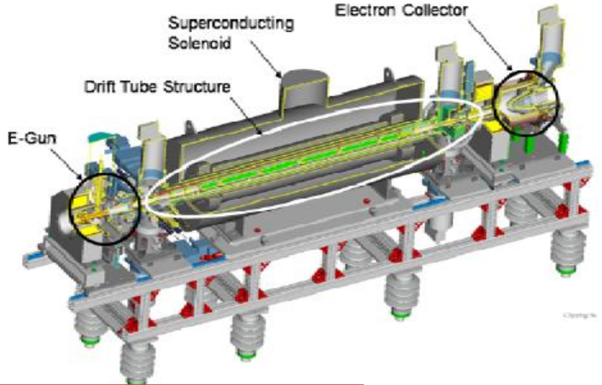

J. Alessi et al, RSI 81(2010)02A509

Design parameters for EBIS

Electron beam	10A
Magnetic field (solenoid)	5.5T
Trap length	1.5m
Vacuum	$<10^{-10}$ Torr
Total extracted charge/pulse	$5x10^{11}$ (80nC)
Output energy	17keV/u

RHIC-EBIS II

The ion yield vs. electron beam current showed twice the output, compared to the BNL Test EBIS, since this EBIS has twice the trap length of the Test EBIS.
Total charge/pulse of ~9x$10^{11}$was achieved at the electron current of ~9A

Table 2: Intensities measured after the 73° dipole

	Ions per pulse	Charges per pulse
He 1+	67 x 10^{9}	6.7 x 10^{10}
Ne 5+	5.5 x 10^{9}	2.7 x 10^{10}
Fe 20+	1.7 x 10^{9}	3.4 x 10^{10}
Au 32+	0.92 x 10^{9}	2.9 x 10^{10}

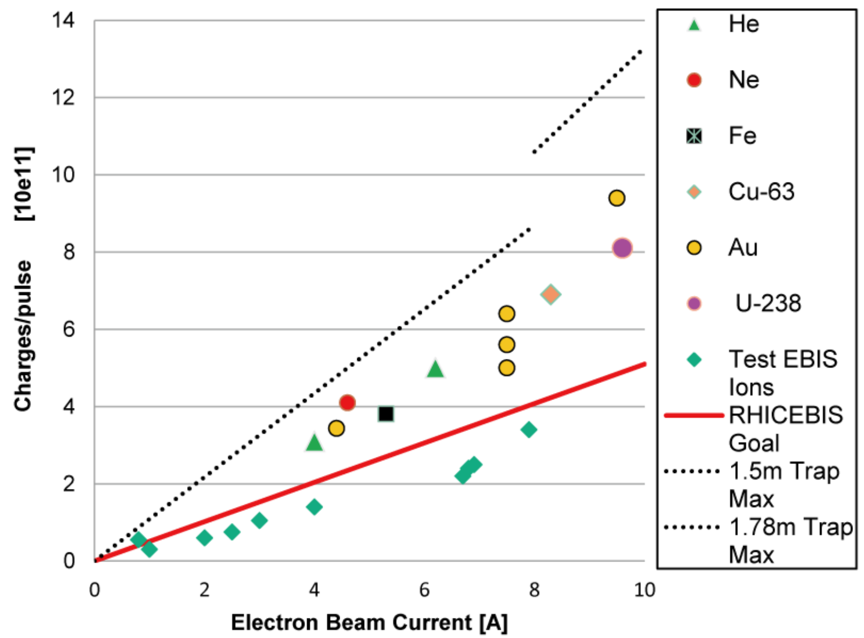

A TOF spectrum of the extracted ion beam with and without Au external ion injection

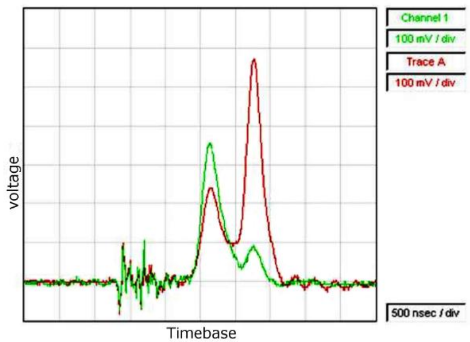

A. Pikin et al, Proc. of INT. SYMP. ON ELECTRON BEAM ION SOURCES AND TRAPS

E. Beebe et al, HIAT2012

RHIC EBIS performance

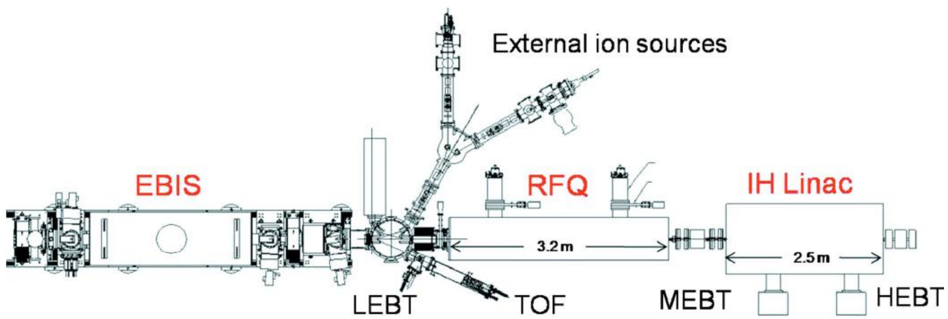

FIG. 1. (Color online) Schematic of the EBIS preinjector front end.

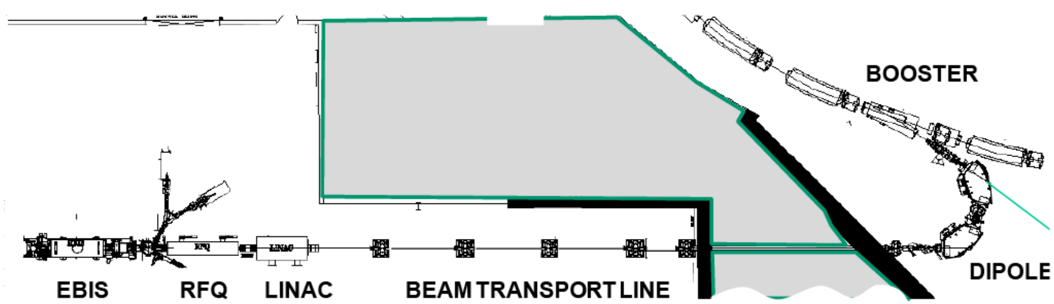

Figure 1: Schematic of the EBIS-based heavy ion preinjector

J. Alessi et al, PAC'11

RHIC EBIS performance

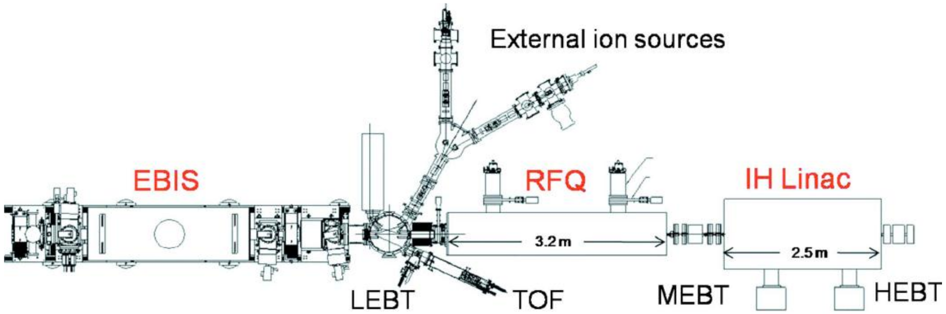

FIG. 1. (Color online) Schematic of the EBIS preinjector front end.

Table 1: Preinjector Parameters

Ions	He – U
Q / m	≥1/6
Current	> 1.5 emA
Pulse length	10–40μs (for few-turn injection)
Rep rate	5 Hz
EBIS output energy	17 keV/u
RFQ output energy	300 keV/u
Linac output energy	2 MeV/u
Time to switch species	1 second

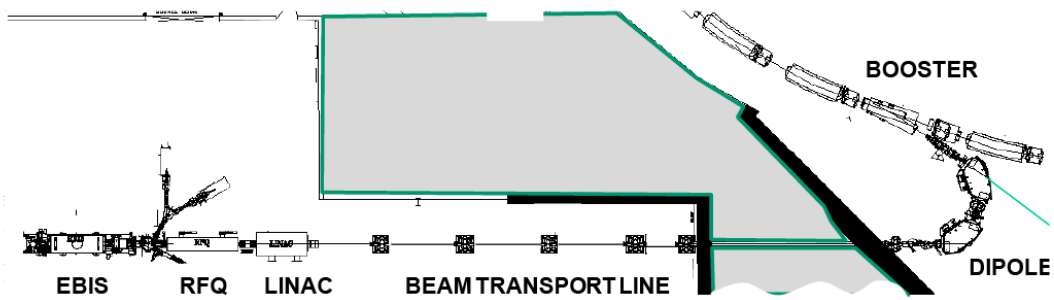

Figure 1: Schematic of the EBIS-based heavy ion preinjector

Table 3: Parameters for helium, gold and iron ions demonstrated for CD-4.

Parameter	He^{+1}	Au^{+32}	Fe^{+20}
q/m	0.25	0.162	0.357
Platform Voltage (kV)	68	104	47.6
RFQ Power (kW)	40	95	20
Linac Power (kW)	75	180	37
Dipole Current (A)	1415	2270	1030
Pulse Length (μs)	20	20	36
Rep. Rate (Hz)	1	1	1
Intensity (10^8) ions/pulse	1250	3.7	4.75
Energy (MeV/u)	2	2	2
Transmission,	75	90*	60*

RFQ input to middle of bend (*=inferred, due to multiple charge states)

J. Alessi et al, PAC'11

Instability (EBIS)

Despite the success using an EBIS in the application, it has reported that it has some limitation of the behaviour.

In 1990's, Donets reported the anomalous behaviour that might limit EBIS performance.

One of the explanations is the existence of plasma instabilities. The instabilities associated with the beam current, electron beam and trapped ions were intensively studied. It was observed that the effective ionization rate was reduced and radial ion current was increased with the instabilities. It should affect the stability of the beam.

To further improve the performance. It is important to study the instabilities experimentally, theoretically with using the simulation code.

Electron beam stability limit

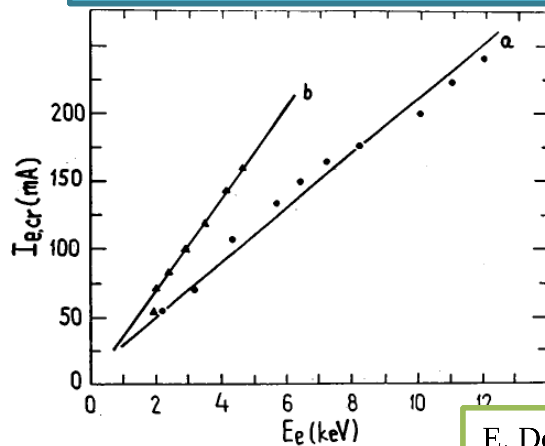

E. Donets RSI 69(1998)614

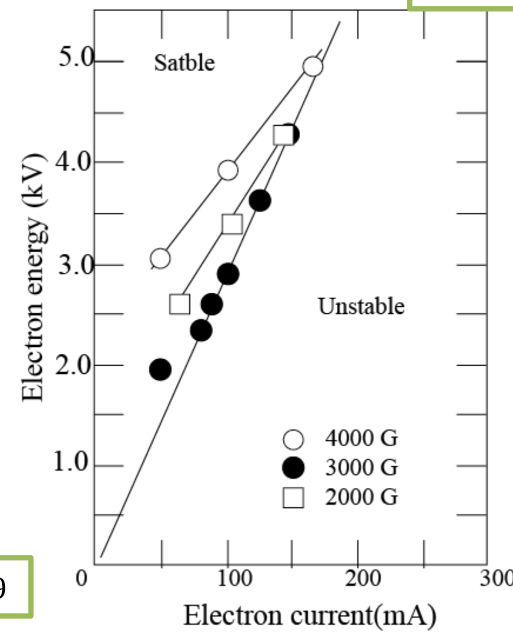

M. Levine et al, NIM A237(1985)429

Next step I (Tandem EBIS)

Additional SC-solenoid coil

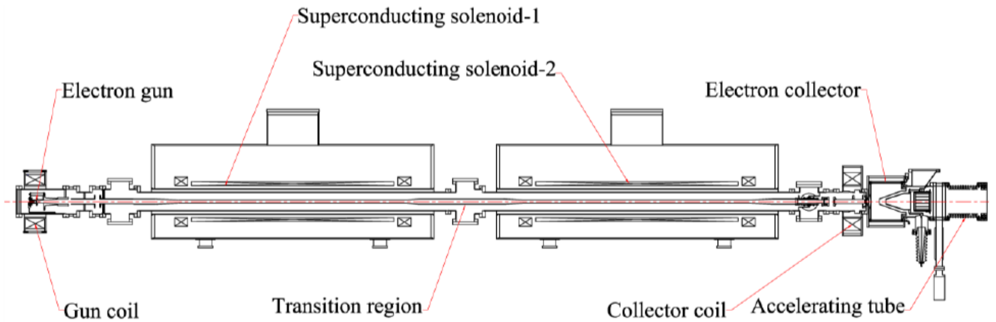

Fig. 1. Schematic of the Tandem EBIS.

It can make to double the EBIS intensity using the existing units: electron gun, electron collector, extraction/injection ion optics, and ion injection system.

A. Pikin et al, HIAT2012, p101

Next step I (Tandem EBIS)

Additional SC-solenoid coil

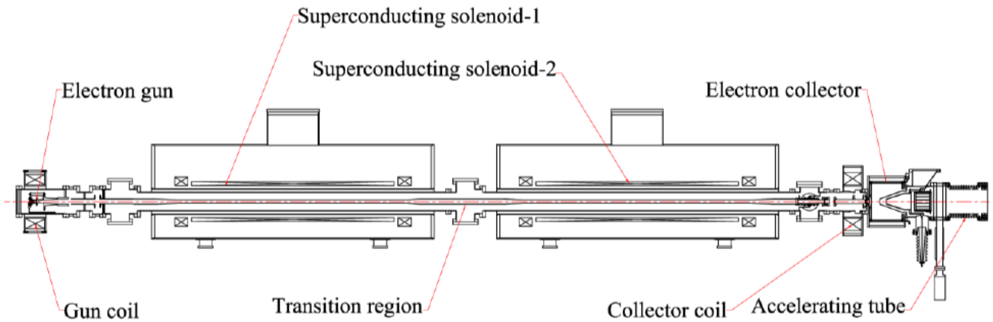

Fig. 1. Schematic of the Tandem EBIS.

trap and two pre-extraction traps is presented in Fig. 2.

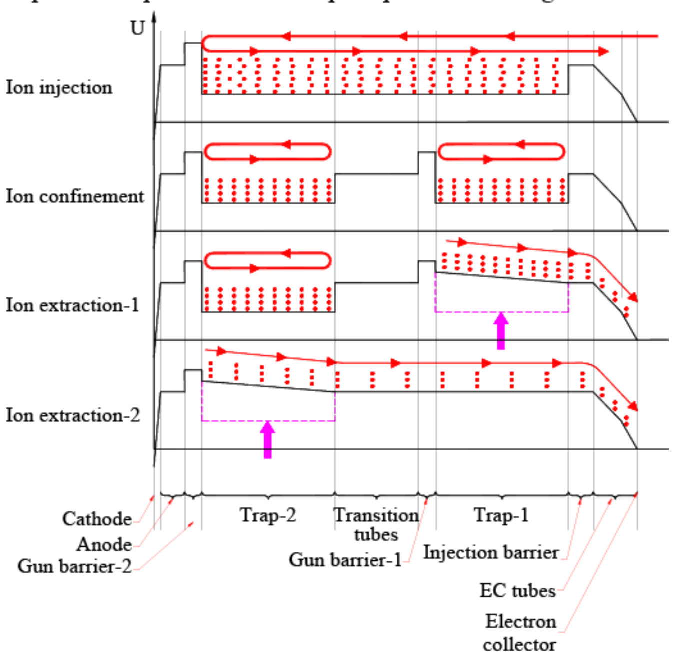

It can make to double the EBIS intensity using the existing units: electron gun, electron collector, extraction/injection ion optics, and ion injection system.

The longitudinal energy spread and transverse emittance growth resulting from a fast ion extraction should be minimizing to match the RHIC requirements

A. Pikin et al, HIAT2012, p101

Next step II (ESIS)

Donets proposed so-called reflex mode of EBIS.

This ion source has specially designed electron gun and electron reflector which allows the multiple use of the electron beam.

The electron string ion source (ESIS) is based on a specially designed electron gun and an electron reflector that allows multiple uses of beam electrons.

At some conditions the electron can be reflected hundred times.

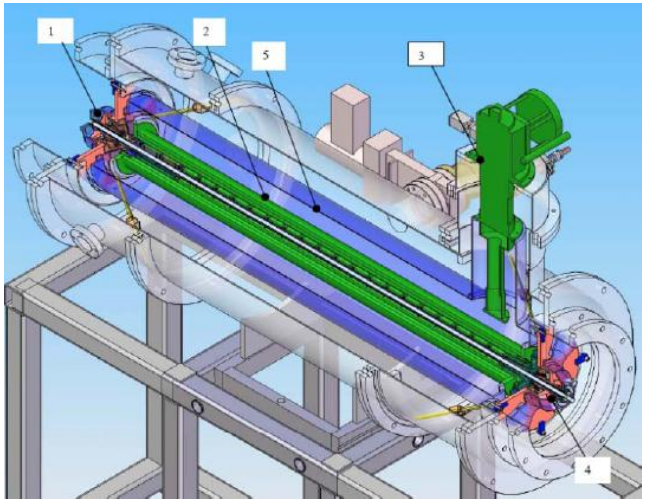

D. Donets et al, EPAC08

Next step II (ESIS)

Donets proposed so-called reflex mode of EBIS.

This ion source has specially designed electron gun and electron reflector which allows the multiple use of the electron beam.

The electron string ion source (ESIS) is based on a specially designed electron gun and an electron reflector that allows multiple uses of beam electrons.

At some conditions the electron can be reflected hundred times.

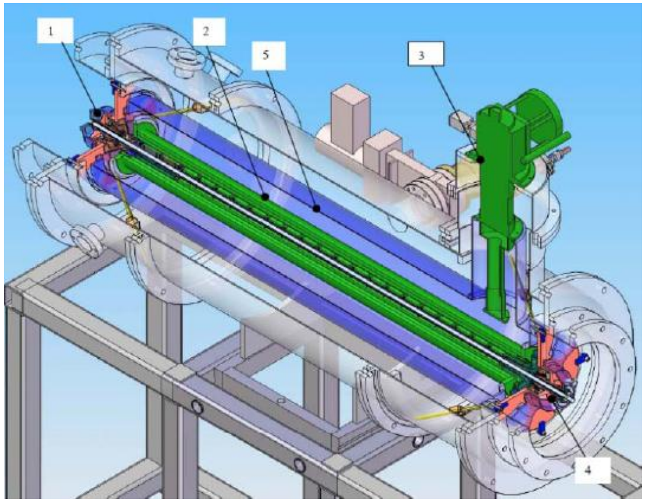

Effect of ion-ion collision cooling

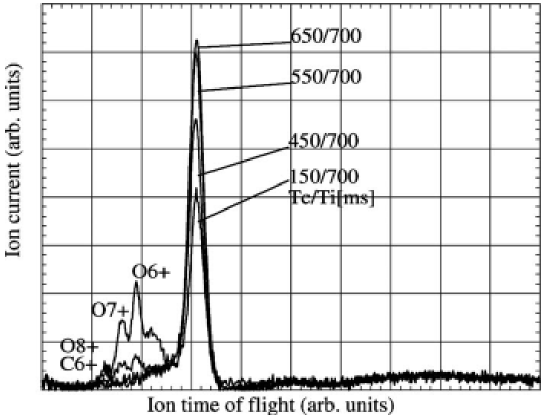

Ar^{16+} 200 eμA
Fe^{24+} 150 eμA
Beam pulse: 8 μs
Injected into JINR synchrotron

D. Donets et al, EPAC08

Ion sources for Pulsed beam production

2.2 **Laser ion source (LIS)**

(I)Physics
(II)CERN LIS
(III)DPIS

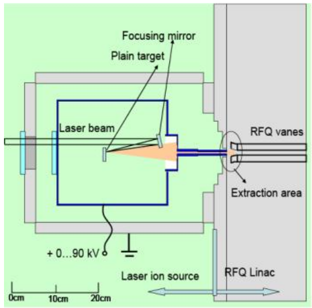

Source geometry

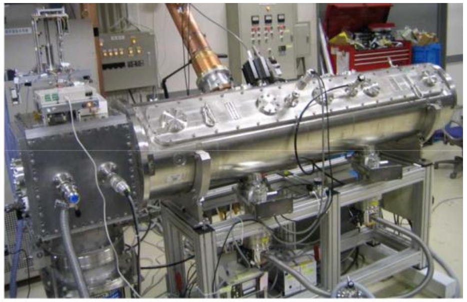

DPIS in RIKEN

Laser plasma

The main energy transfer from the laser to the plasma is inverse bremsstrahlung for the laser power density up to 10^{13} W/cm^2.

Inverse bremsstrahlung absorption coefficient

$$K_{ab} = \frac{v(n_{cr})L_h}{c}$$

$$v(n_{cr}) = 4\sqrt{2\pi}Ze^4\Lambda_{ei}n_{cr}/3m_e(kT_e)^{2/3}$$

Based on it, for laser ion source design, the laser which has the power density of 10^{10}~several 10^{13}W/cm^2, wave length >1000nm and pulse with of 1~100ns was used in many laboratories. In that case, the experimental results and theoretical calculation show the absorption efficiency is from 70 to 90%.

Absorption efficiency

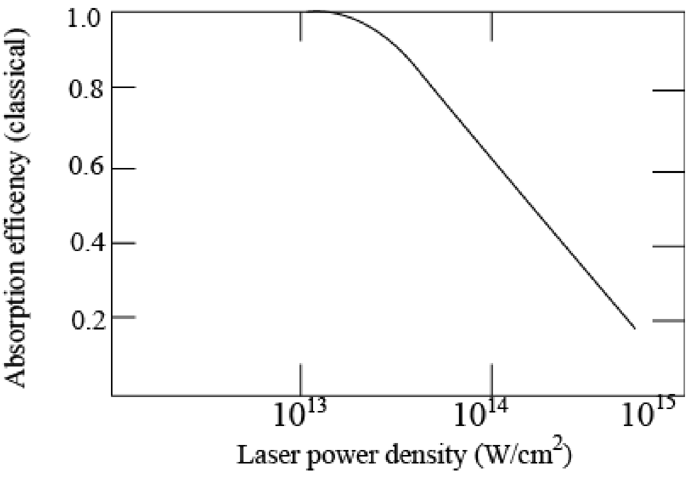

Laser plasma

The main energy transfer from the laser to the plasma is inverse bremsstrahlung for the laser power density up to 10^{13} W/cm^2.

Inverse bremsstrahlung absorption coefficient

$$K_{ab} = \frac{v(n_{cr})L_h}{c}$$

$$v(n_{cr}) = 4\sqrt{2\pi}Ze^4\Lambda_{ei}n_{cr}/3m_e(kT_e)^{2/3}$$

Based on it, for laser ion source design, the laser which has the power density of 10^{10}~several 10^{13}W/cm^2, wave length >1000nm and pulse with of 1~100ns was used in many laboratories. In that case, the experimental results and theoretical calculation show the absorption efficiency is from 70 to 90%.

Absorption efficiency

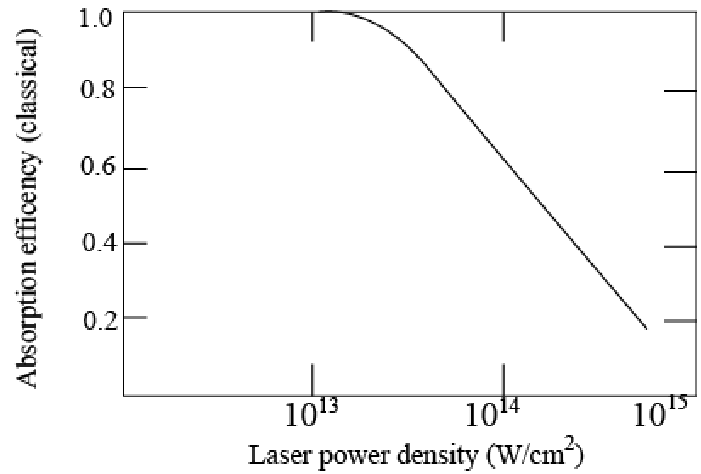

Electron temperature strongly dependent on the laser power density

$$T_e \propto \left(\frac{I^2 m_i}{n_{cr}Z}\right)^{1/3}$$

For this reason, average charge state is also depend on the power
(higher power highly charged heavy ions)

RIKEN NiSHiNA CENTER

Pulse width and beam current

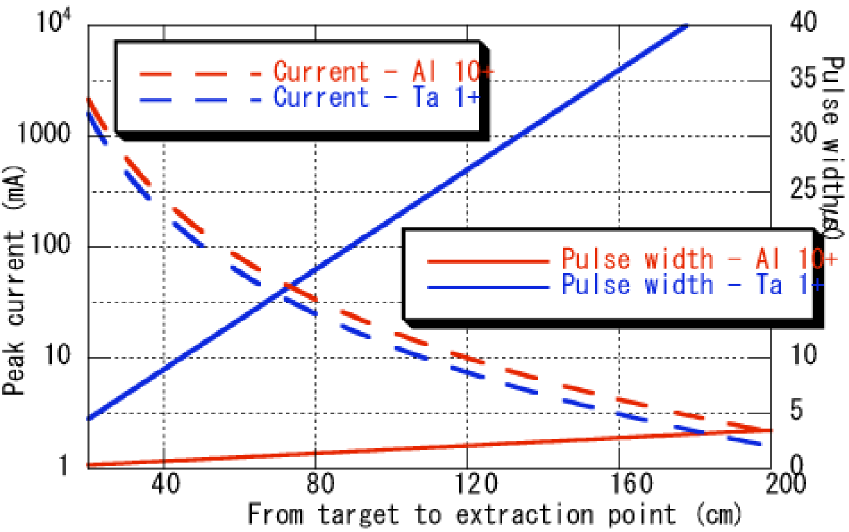

$$\tau_{1/2}=2\times 10^{6} P^{-0.43} L$$

The pulse width (t) and beam intensity(I) are defined as, $t \propto L, I \propto L^{-3}$, where L is the distance from the target to the extraction system.

It is easy to increase the pulse width with increasing the drift distance.

Injected current to the RFQ becomes small, because the intensity is proportional to L^{-3} as shown in the formula described above.

Pulse width and beam current

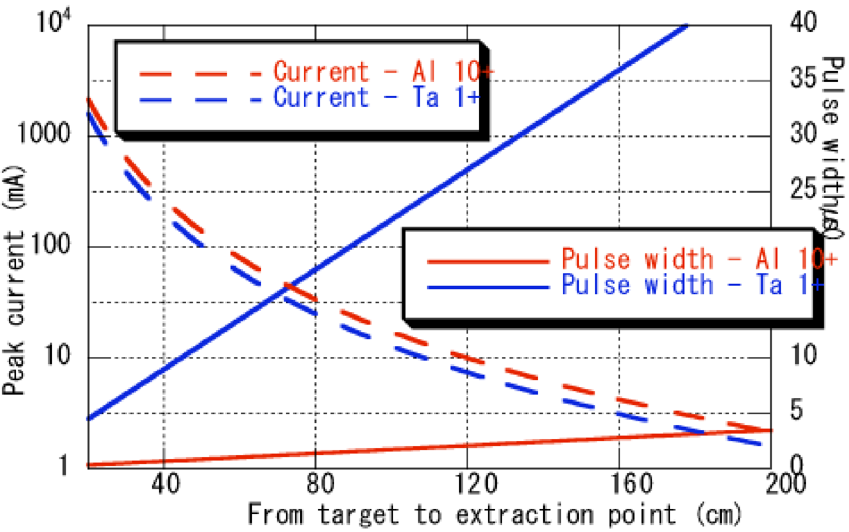

$$\tau_{1/2}=2\times 10^{6} P^{-0.43} L$$

The pulse width (t) and beam intensity(I) are defined as, $t \propto L, I \propto L^{-3}$, where L is the distance from the target to the extraction system.

It is easy to increase the pulse width with increasing the drift distance.

Injected current to the RFQ becomes small, because the intensity is proportional to L^{-3} as shown in the formula described above.

Recombination effect

$$R_{3B} \cong 10^{-26} Z^{3} \frac{N_e}{T^{4.5}}$$

Thus to maximize the highly charged ion beam, R_{3B} should be minimized
High temperature and low-density plasma is desirable.

CERN LIS

100J CO_2 Laser

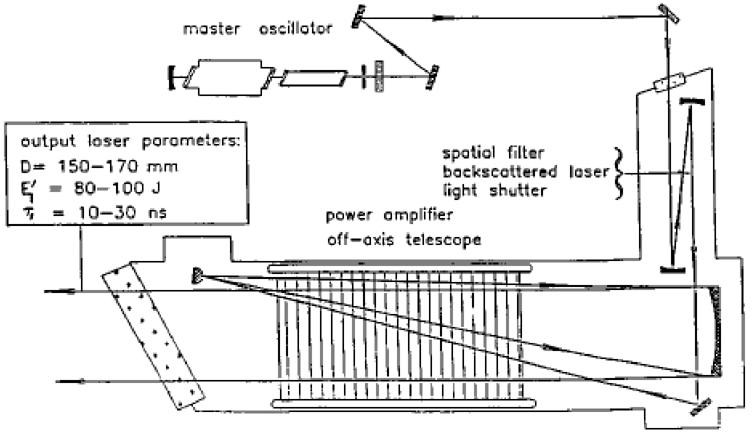

Parameters of CERN LIS for LHC

TABLE I. Specification parameters of the laser ion source (laser system scheme: master–oscillator/power amplifier).

Parameter	Value
Total laser energy	$\geqslant$100 J
useful laser energy	$\geqslant$80 J
Laser pulse duration	30–50 ns
Diameter of the focal spot	170–250 μm
Laser power density	(0.8–1.2) 10^{13} W/cm^2
Laser beam diameter	160 mm
Focal length of the focusing mirror	200–300 cm
Incident angle at the target	$<5°$
Plasma expansion length	200–260 cm
Total extraction current density	8.8 mA/cm^2
Diameter of the extraction hole	34 mm
Number of Pb^{208} particles with $Z=25+$	1.4×10^{10}
Ion pulse length	1.5; 3; 6 μs
Emittance of extracted Pb^{208} ion beam ϵ (4 rms at 9.6 keV/u)	44 mm mrad
Extraction potential	80 kV
Source repetition rate	1 Hz
Energy spread dE/E	$<\pm2.5\%$
Number of LIS operation cycles between interventions	2×10^6

Chamber and extraction system

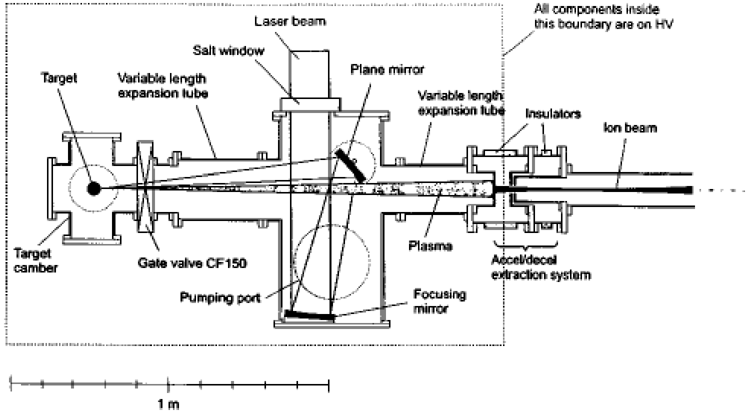

S. Kondrashev et al, EPAC04

CERN LIS

A 100 J/1 Hz CO2-laser system has been built for the CERN LIS.
Stable operation has been demonstrated during a few hours

Pb^{27+} ion beams (16% of total ion flux) was obtained for laser power density of $3 \cdot 10^{13}$ W/cm^2
.
The ion beam has been extracted at 105 kV in 1 Hz rep-rate without vacuum problems or extraction system breakdowns.

Setup for CERN LIS

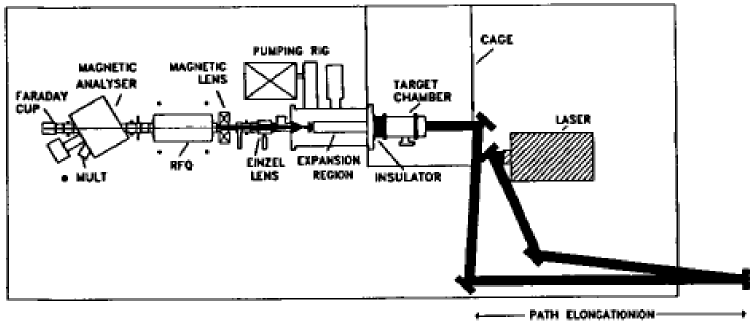

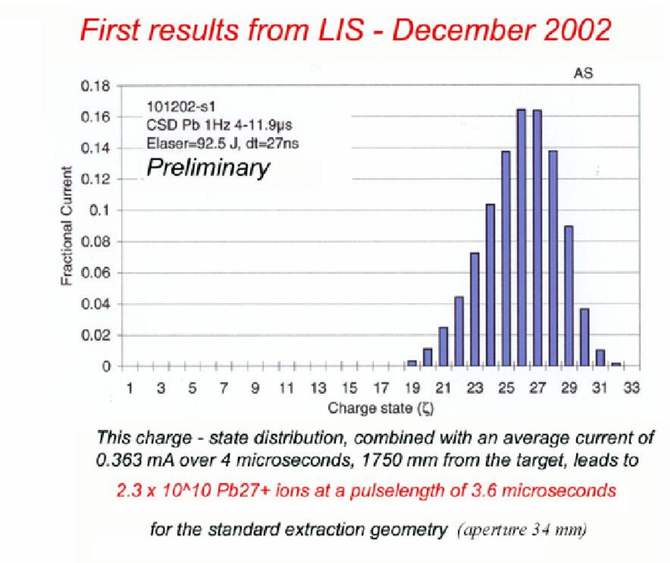

S. Kondrashev et al, EPAC04

Direct plasma injection scheme (DPIS)

The laser ablation plasma has very high density and has initial expanding velocity.

We can transport the intense ion beam under the plasma condition (neutralization) into the first stage accelerator.

The direct plasma injection scheme (DPIS) was proposed.

Direct plasma injection scheme lay-out

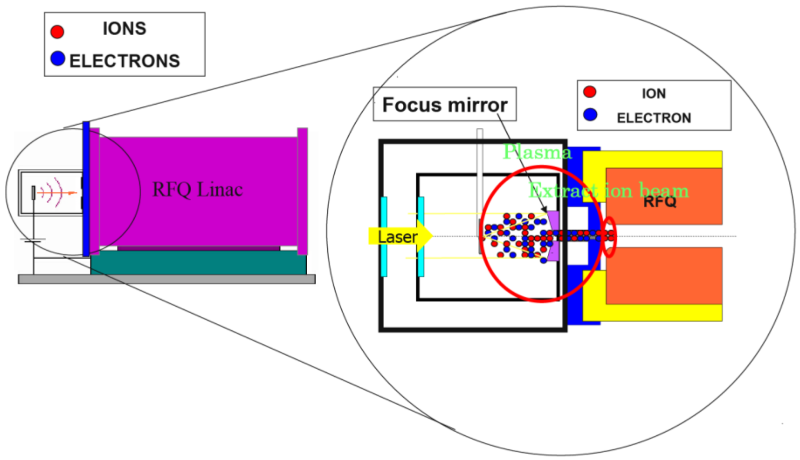

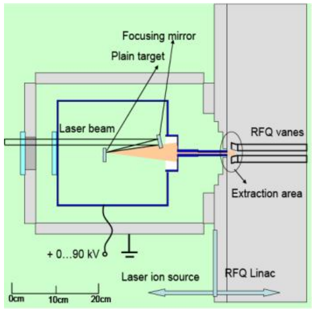

Source geometry

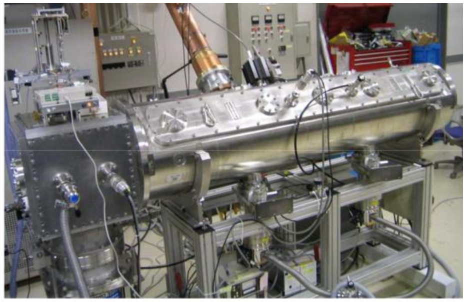

DPIS in RIKEN

Direct plasma injection scheme (DPIS)

The laser ablation plasma has very high density and has initial expanding velocity.
We can transport the intense ion beam under the plasma condition (neutralization) into the first stage accelerator.
The direct plasma injection scheme (DPIS) was proposed.

Direct plasma injection scheme lay-out

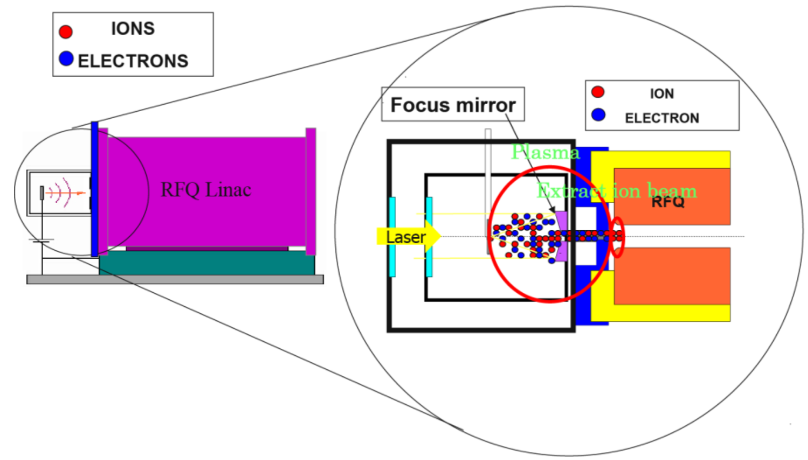

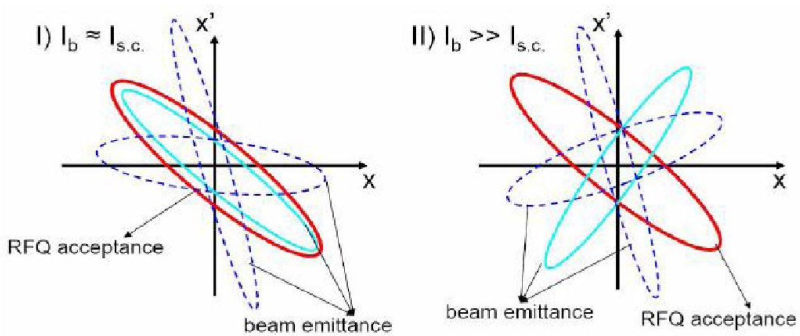

"conventional" LIS   DPIS

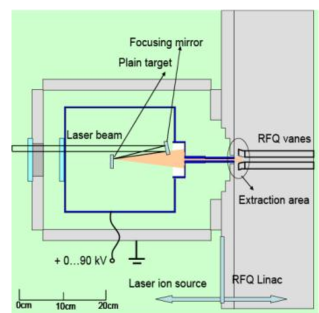

Source geometry

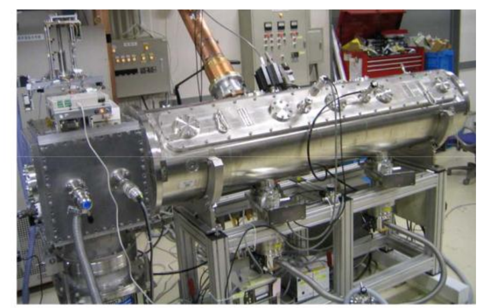

DPIS in RIKEN

Developments of DPIS

The obtained peak current was already more than 9 mA from a carbon graphite target using a 4 J CO_2 laser in the early stage of the test experiment.

After the test experiments, a new RFQ linac was fabricated to accelerate high intensity heavy ion beam (~100mA).

400 mJ Nd-YAG laser was tested to produce fully stripped carbon beam and the measured result showed that accelerated peak current reached up to 17 mA.

In 2005, Intense C beams (>60mA) were accelerated, when using 4J CO_2 laser. they also obtained 70mA of Al ions with 2.3J commercial Nd-YAG laser.

M. Okamura et al, PAC2005

DPIS

Developments of DPIS

The obtained peak current was already more than 9 mA from a carbon graphite target using a 4 J CO_2 laser in the early stage of the test experiment.

After the test experiments, a new RFQ linac was fabricated to accelerate high intensity heavy ion beam (~100mA).

400 mJ Nd-YAG laser was tested to produce fully stripped carbon beam and the measured result showed that accelerated peak current reached up to 17 mA.

In 2005, Intense C beams (>60mA) were accelerated, when using 4J CO_2 laser. they also obtained 70mA of Al ions with 2.3J commercial Nd-YAG laser.

M. Okamura et al, PAC2005

Beam intensity and pulse width stability

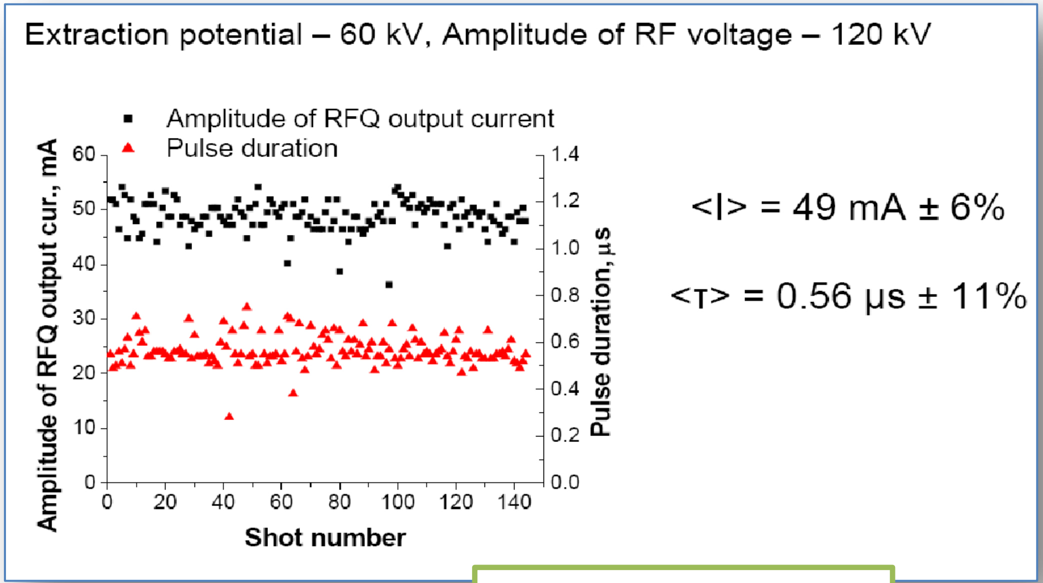

S. Kondrashev et al, HB2006

The pulse width (t) and beam intensity(I) are defined as, $t \propto L, I \propto L^{-3}$
. For this reason, it is easy to increase the pulse width with increasing the drift distance between ion source and RFQ.
However the injected current to the RFQ becomes very small, because the intensity is proportional to L^{-3}

Recently, to minimize the reduction of the current, a solenoid magnet was successfully used for focusing the beam.

Pulse shape with and without magnetic field

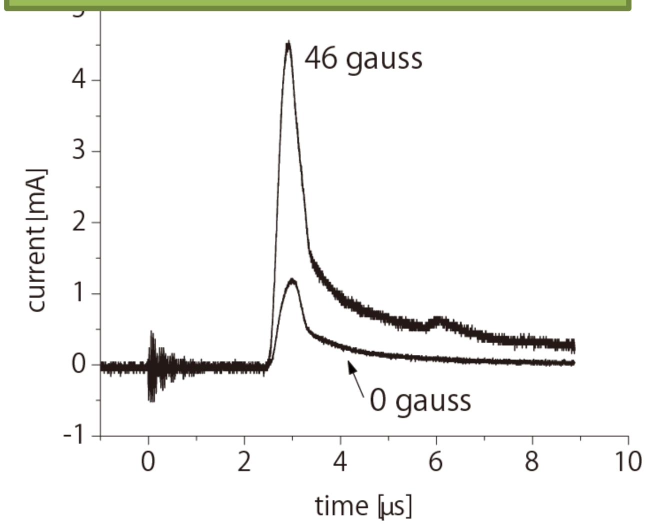

M. Okamura et al, IPAC2010

Pulse height as a function of magnetic field

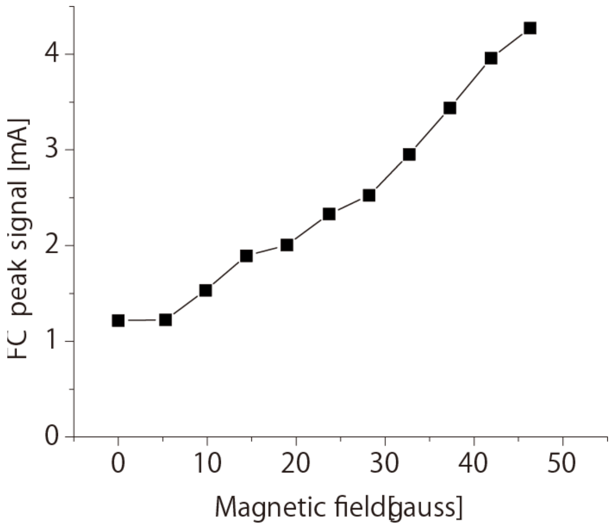

Next step (Application of DPIS)

Compact carbon ion cancer therapy facility in China

Beam test of DPIS is carried out for the first time in China.

The C^{6+} beam (>6mA) is accelerated

The RF power of about 195kW is required to produce the peak beam current

LIS and RFQ

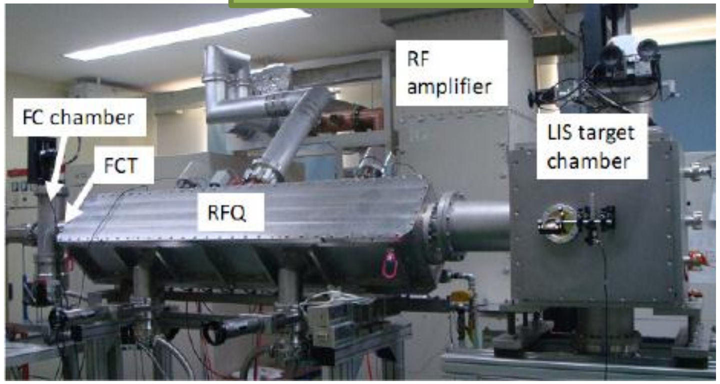

Charge state distribution

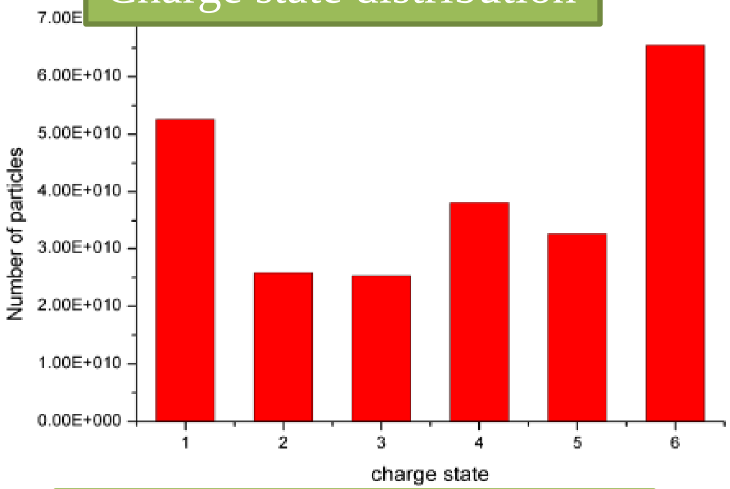

Z. Zhang et al, IPAC2011 MOPC028

Beam intensity as a function of RF power

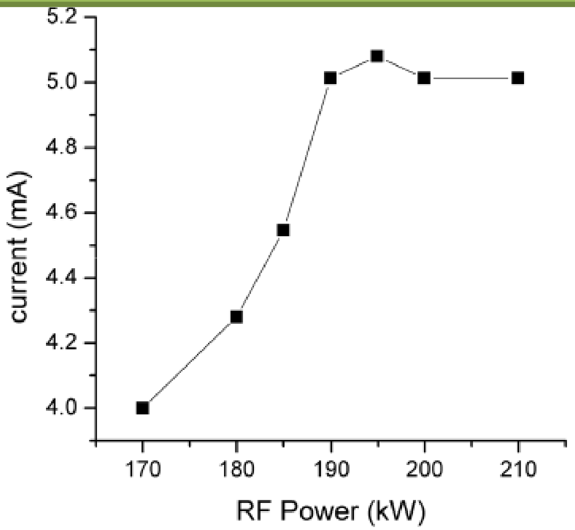

Ion sources for DC beam production

3.1 **Electron cyclotron resonance ion source (ECRIS)**

(I)Physics
(II)SC-ECRISs (VENUS, SECRAL, RIKEN)
(III)What is the limitation of the beam intensity
(RF power, magnetic field,…….)

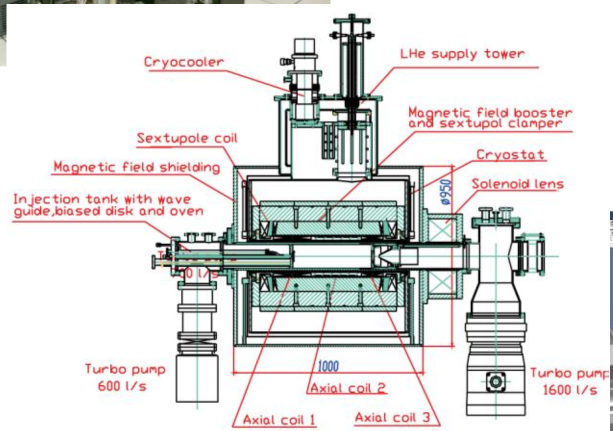

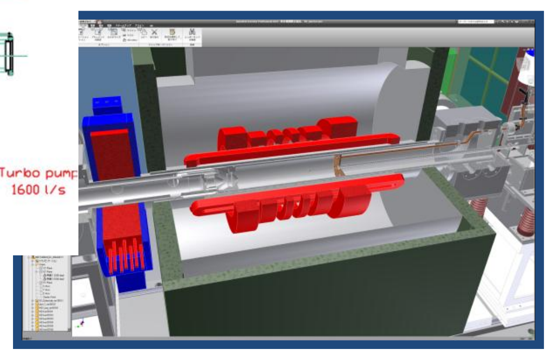

Time evolution of the beam intensity (ECRIS)

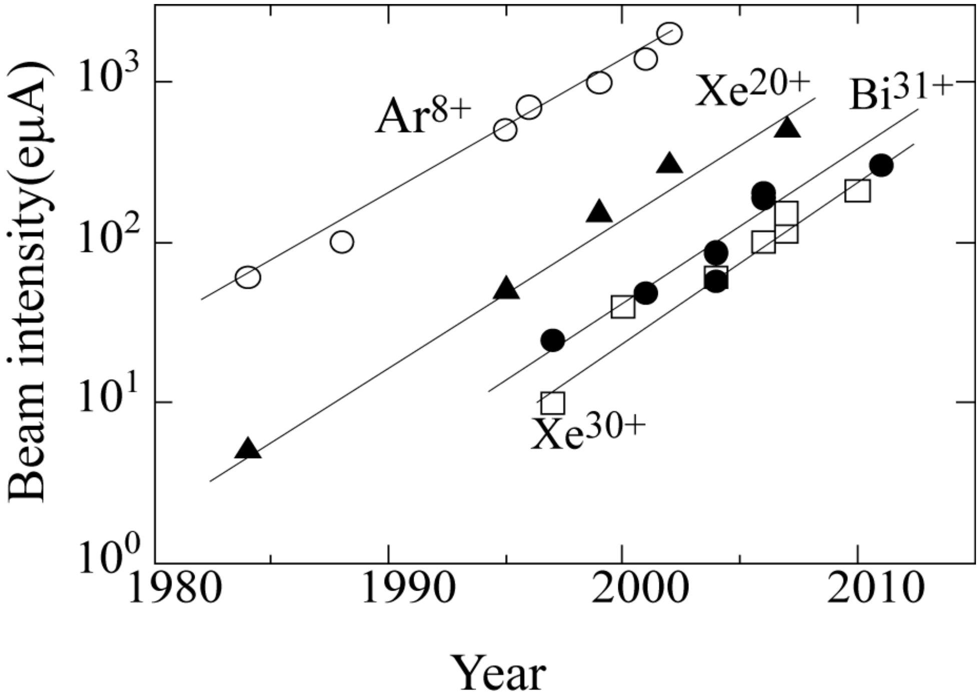

Time evolution of the beam intensity (ECRIS)

Ar^{8+} ~80eμA → 2mA

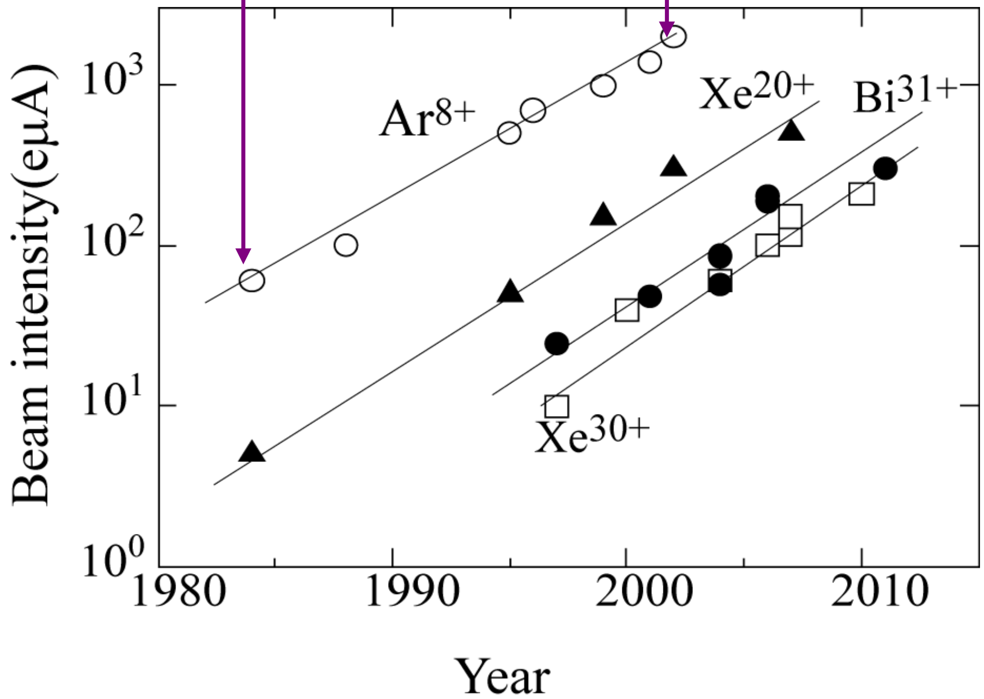

Time evolution of the beam intensity (ECRIS)

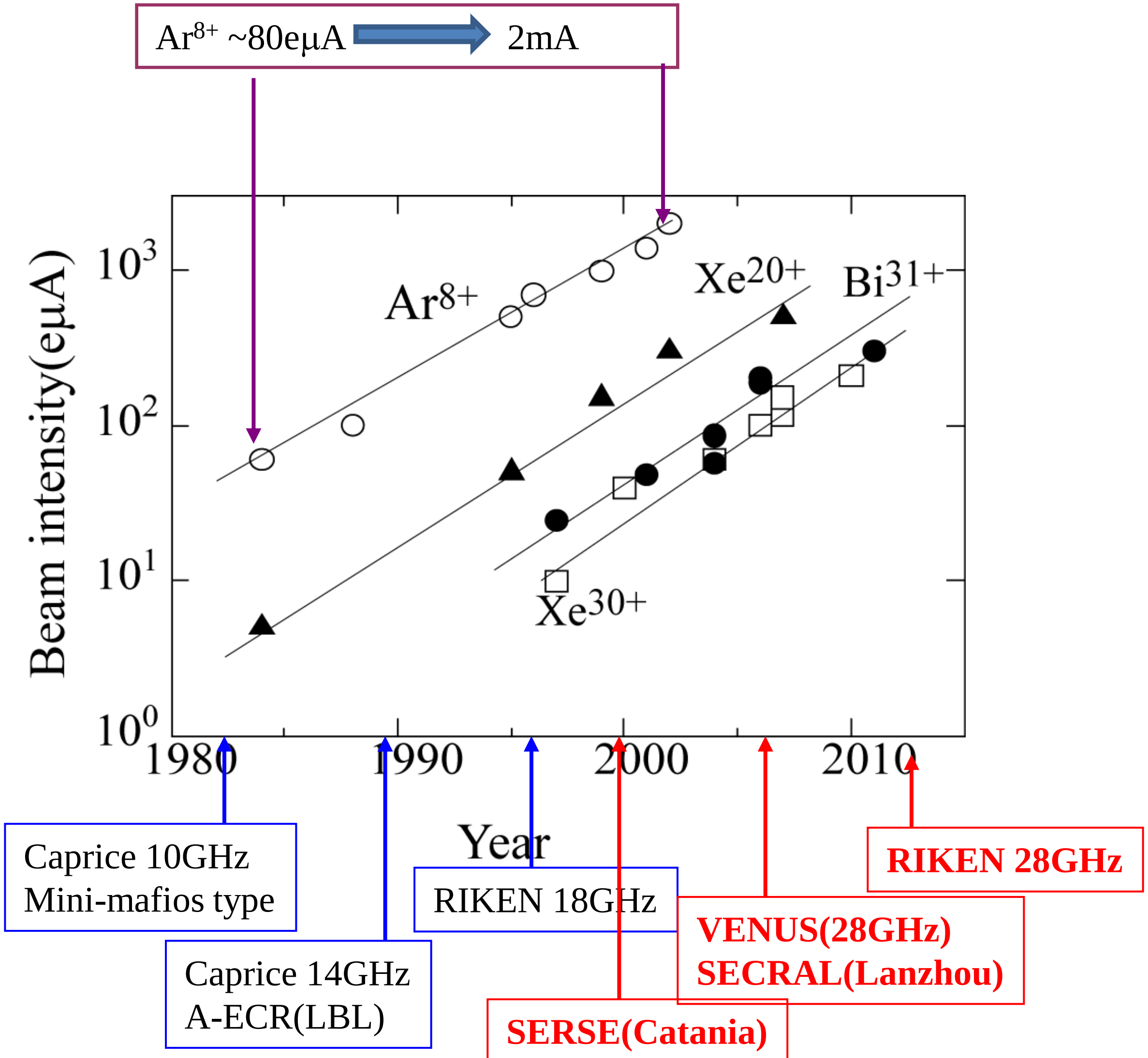

Time evolution of the beam intensity (ECRIS)

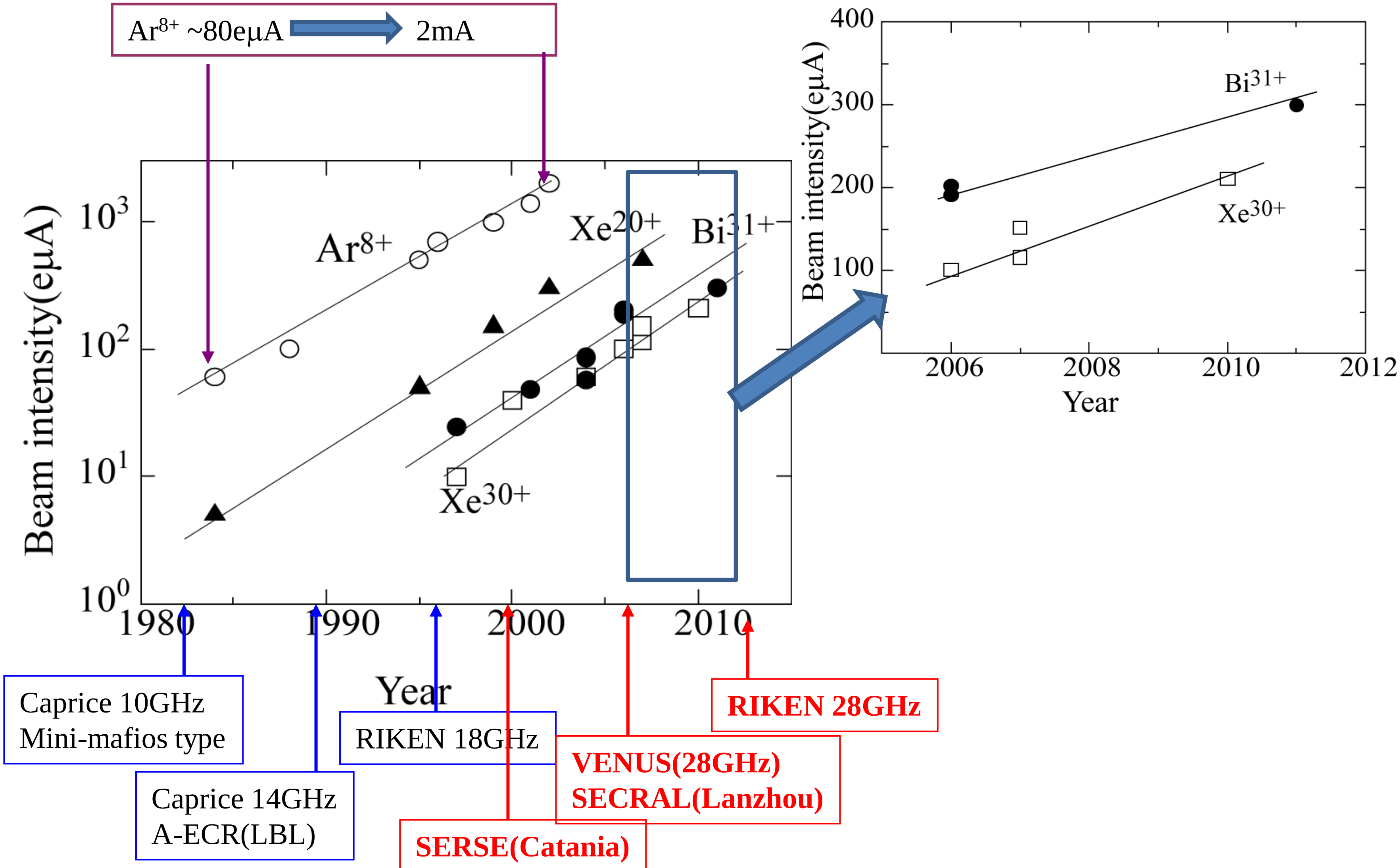

Time evolution of the beam intensity (ECRIS)

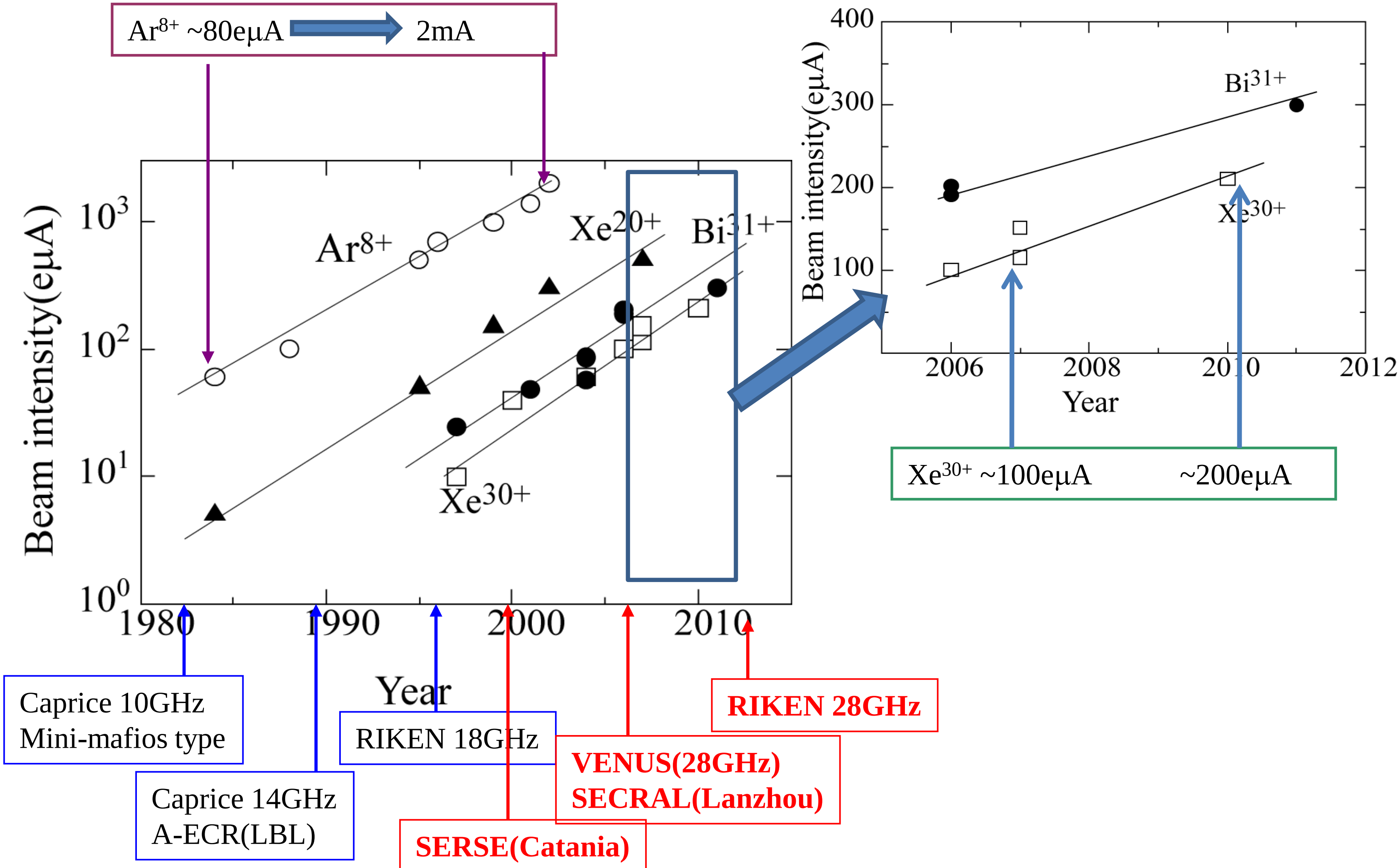

Time evolution of the beam intensity (ECRIS)

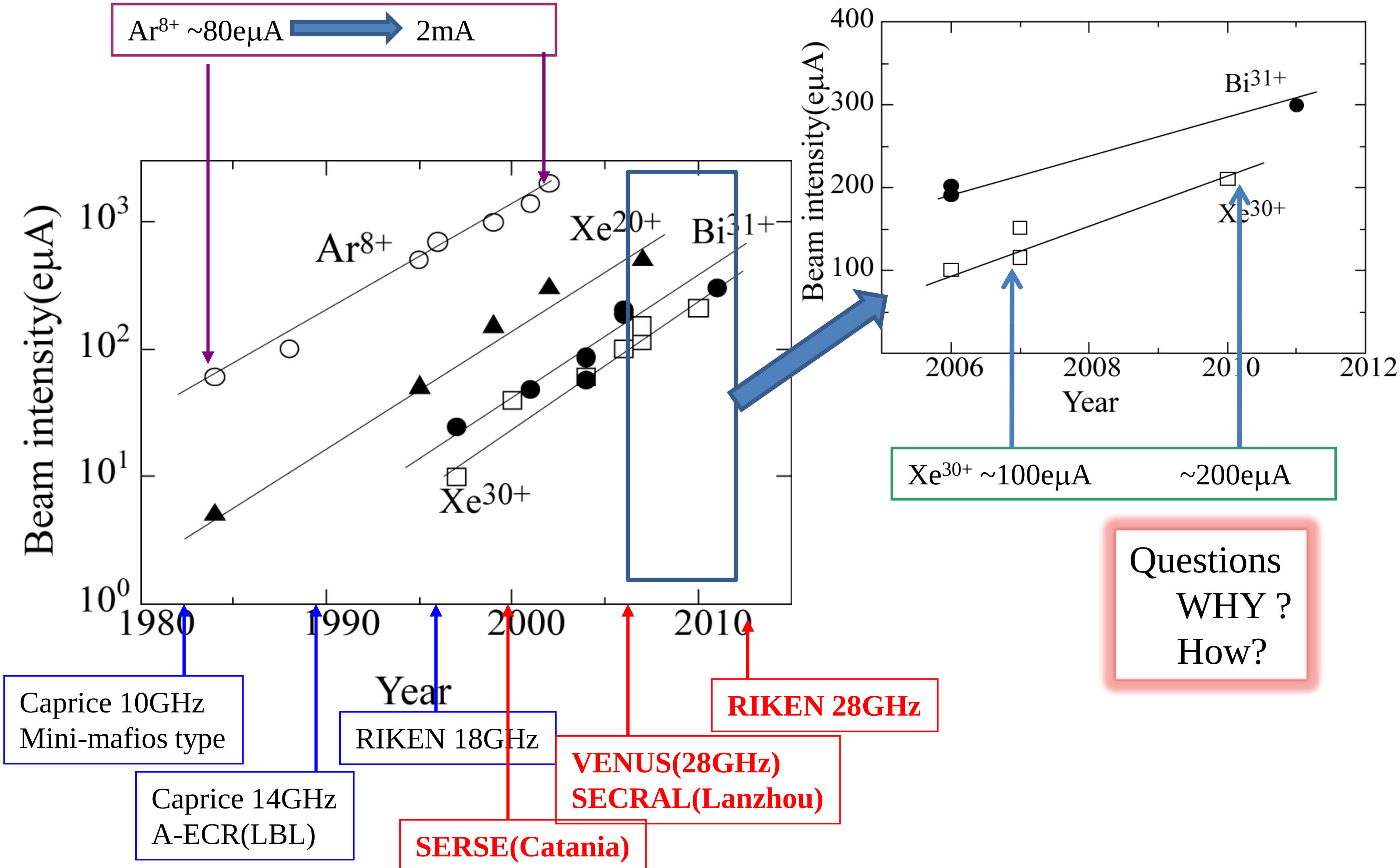

Questions
WHY ?
How?

Magnetic field effect –magnetic mirror-

High B mode operation (B_{inj}>3~4B_{ecr}, Br~2B_{ecr}, B_{ext}<Br, B_{min}~0.6~0.8B_{ecr})

Plasma confinement

B_{inj}/B_{min} (Mirror ratio)

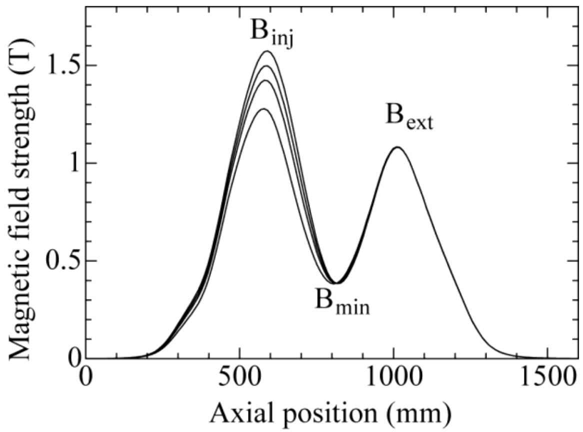

Magnetic field effect –magnetic mirror-

High B mode operation (B_{inj}>3~4B_{ecr}, Br~2B_{ecr}, B_{ext}<Br, B_{min}~0.6~0.8B_{ecr})

Plasma confinement

B_{inj}/B_{min} (Mirror ratio)

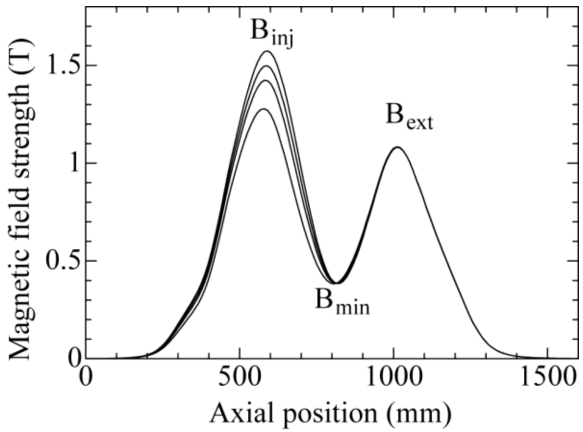

We need high mirror ratio to produce highly charged heavy ions (good plasma confinement), However the beam intensity is saturated B_{inj}>3~4B_{ecr}

Simulation (Fokker-Planck eq.)

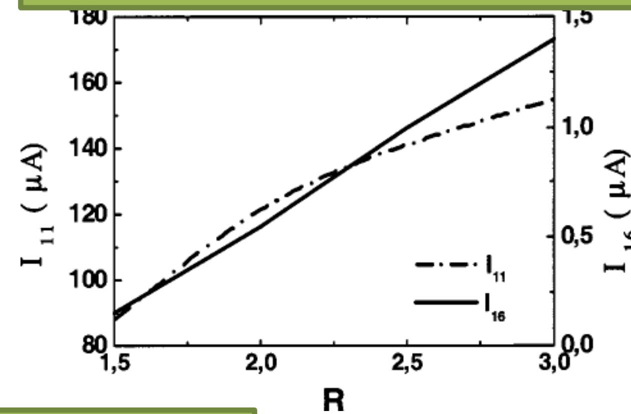

Experimental

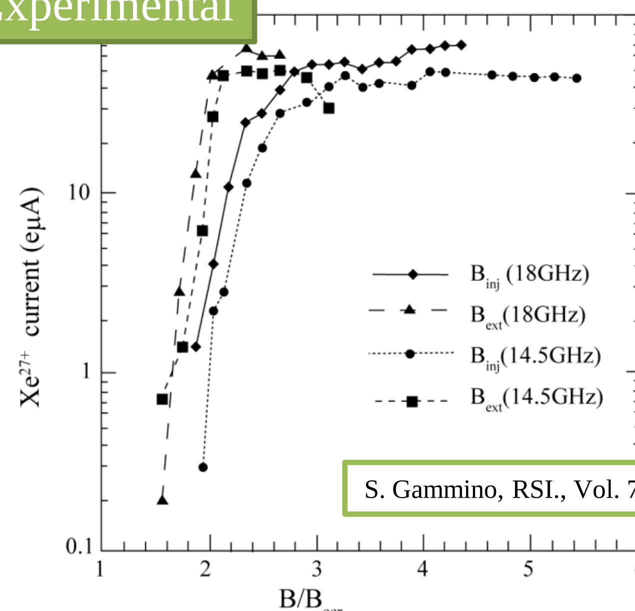

S. Gammino, RSI., Vol. 70, 1999,3577

Magnetic field effect- ECR zone-

B_{min} affects ECR zone size and field gradient

Microwave absorption (ECR zone effect)

Energy transfer from microwave to electron at ECR zone

Y. Kawai et al, Phys. Letter A371(2007)307

$$W_{power} = \left(\frac{\pi n e^2 E^2}{m\omega \left(\frac{dB}{dZ}\right)} \right) S_{ecr}$$

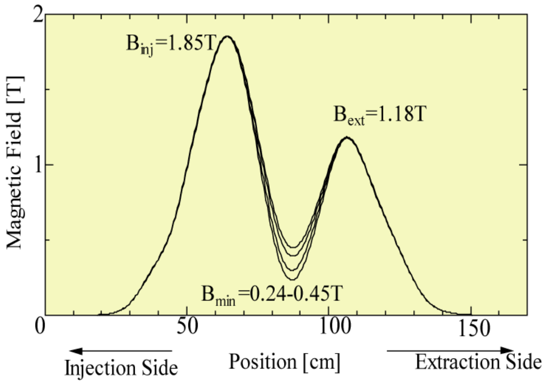

Magnetic field effect- ECR zone-

B_{min} affects ECR zone size and field gradient

Energy transfer from microwave to electron at ECR zone

Microwave absorption (ECR zone effect)

Y. Kawai et al, Phys. Letter A371(2007)307

$$W_{power} = \left(\frac{\pi n e^2 E^2}{m\omega \left(\frac{dB}{dZ}\right)} \right) S_{ecr}$$

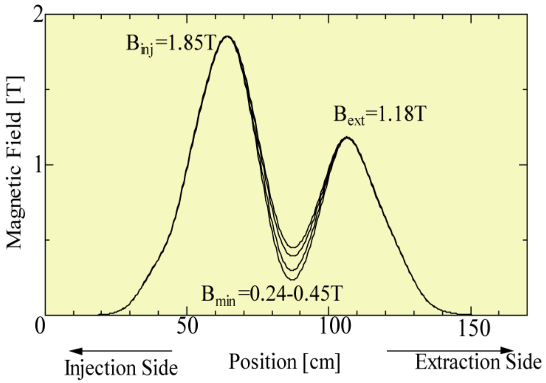

Magnetic field gradient

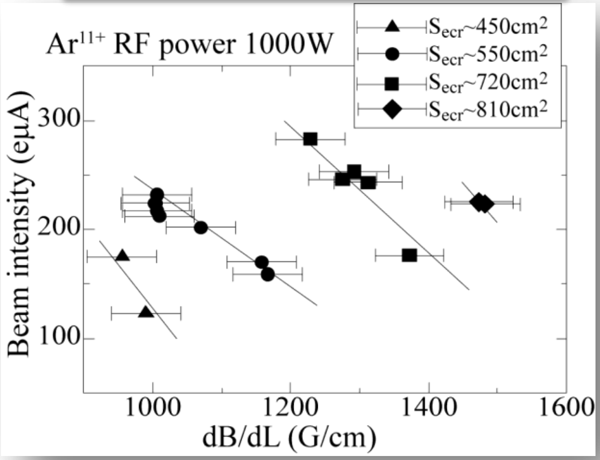

Magnetic field effect- ECR zone-

B_{min} affects ECR zone size and field gradient

Energy transfer from microwave to electron at ECR zone

Microwave absorption (ECR zone effect)

Y. Kawai et al, Phys. Letter A371(2007)307

$$W_{power}=\left(\frac{\pi n e^2 E^2}{m\omega\left(\frac{dB}{dZ}\right)}\right)S_{ecr}$$

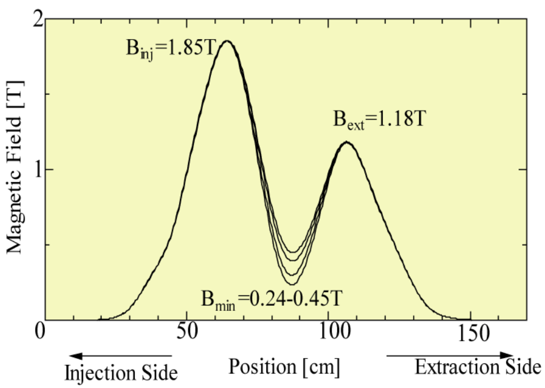

Magnetic field gradient

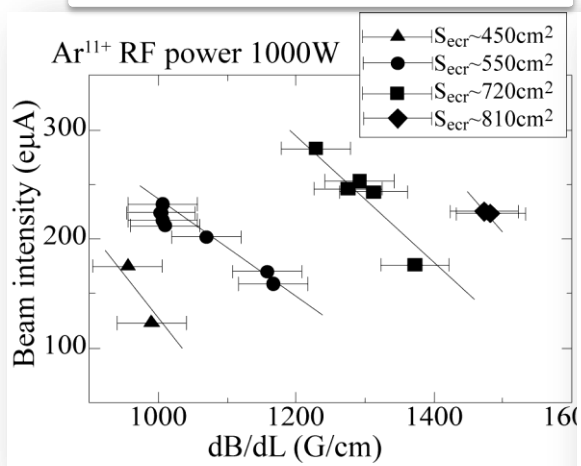

ECR zone size

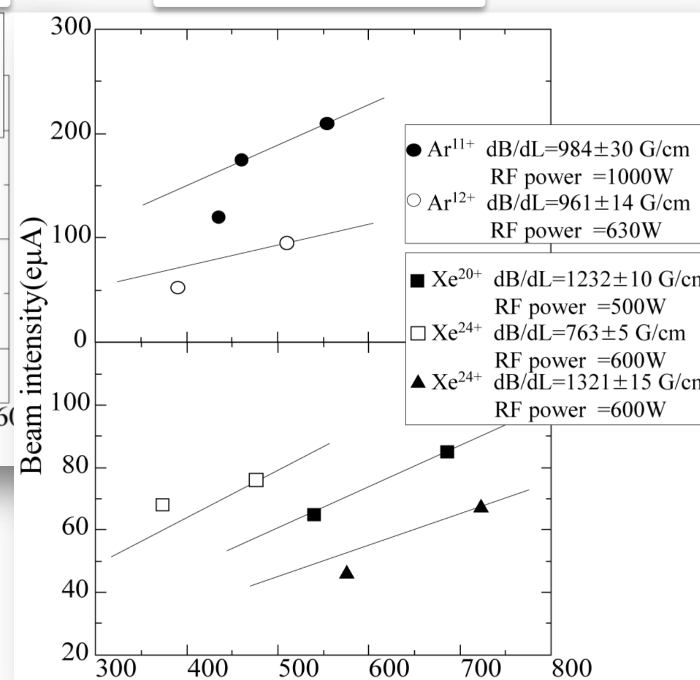

Beam intensity increases with decreasing the magnetic field gradient and/or increasing the ECR zone size

Frequency effect

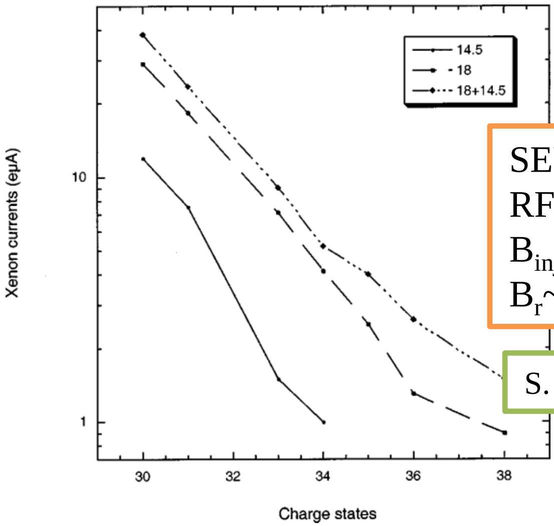

SERSE
RF power 1.8kW
B_{inj}~3.5B_{ecr},B_{min}~0.8B_{ecr},B_{ext}~2B_{ecr}
B_r~2B_{ecr}

S. Gammino, RSI., Vol. 70, 1999,3577

Frequency effect

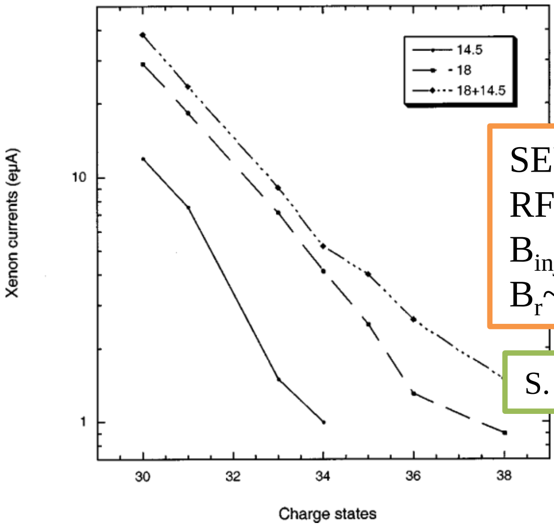

SERSE
RF power 1.8kW
B_{inj}~3.5B_{ecr},B_{min}~0.8B_{ecr},B_{ext}~2B_{ecr}
B_r~2B_{ecr}

S. Gammino, RSI., Vol. 70, 1999,3577

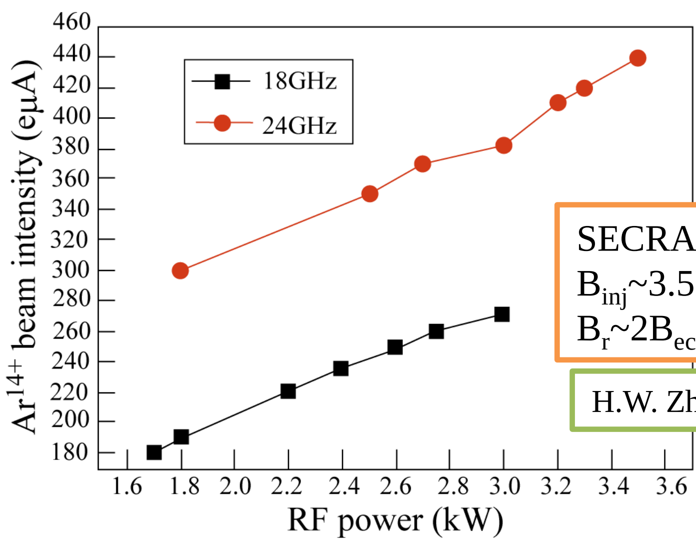

SECRAL
B_{inj}~3.5B_{ecr},B_{min}~0.8B_{ecr},B_{ext}~2B_{ecr}
B_r~2B_{ecr}

H.W. Zhao et al, RSI 81(2010)02A202

Frequency effect

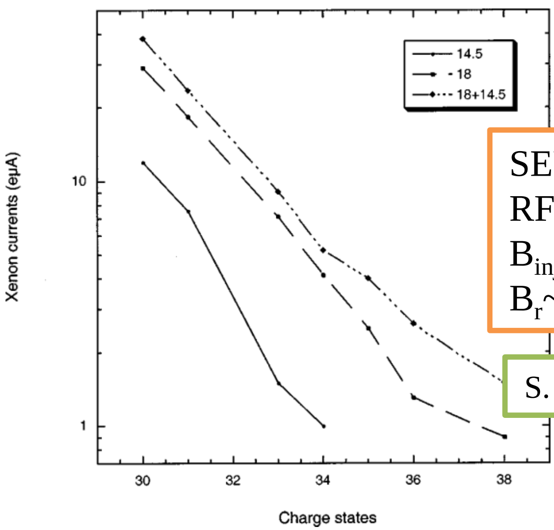

SERSE
RF power 1.8kW
B_{inj}~3.5B_{ecr},B_{min}~0.8B_{ecr},B_{ext}~2B_{ecr}
B_r~2B_{ecr}

S. Gammino, RSI., Vol. 70, 1999,3577

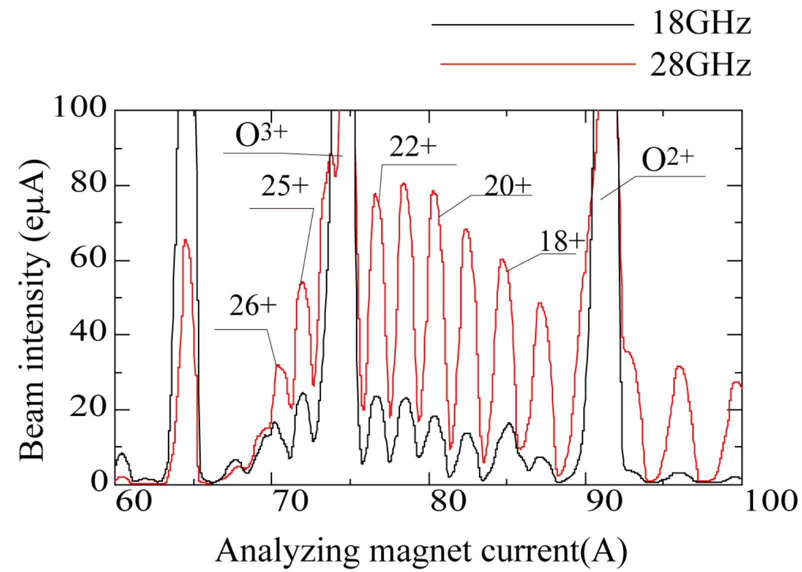

	B_{inj}	B_{min}	B_{ext}	B_r
28GHz	3.15	0.62	1.83	1.86T
18GHz	2.1	0.4	1.18	1.2T (18/28)

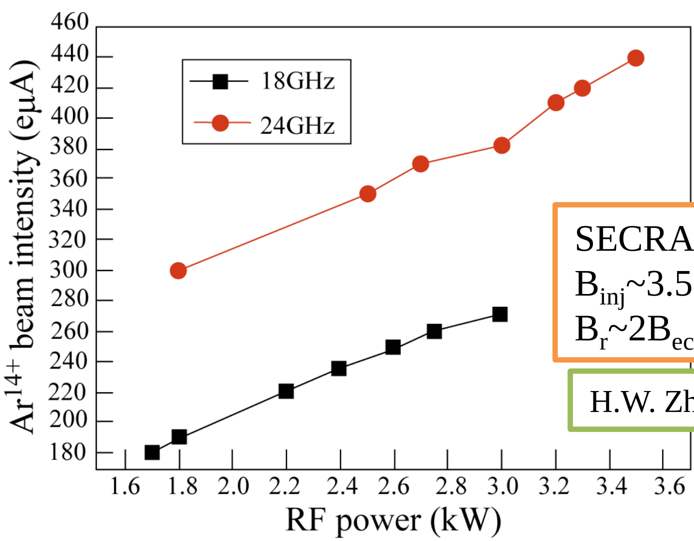

SECRAL
B_{inj}~3.5B_{ecr},B_{min}~0.8B_{ecr},B_{ext}~2B_{ecr}
B_r~2B_{ecr}

H.W. Zhao et al, RSI 81(2010)02A202

Frequency effect (theoretical calculation)

Fokker -Planck equation

Collision term

HF term

Source term

$$\frac{\partial f_e}{\partial t} = C(f_e) + Q(f_e) + S(f_e)$$

$$Q = \frac{1}{\mathrm{v}^2}\frac{\partial}{\partial \mathrm{v}}\left(\mathrm{v}^2 D_{\mathrm{vv}}\frac{\partial f_e}{\partial \mathrm{v}}\right) + \frac{1}{\mathrm{v}^2}\frac{\partial}{\partial \mu}\left((1-\mu^2) D_{\mu\mu}\frac{\partial f_e}{\partial \mu}\right)$$

$$D_{\mathrm{vv}} = D = \frac{4}{3}\pi\left(\frac{eE}{2m_e}\right)^2\frac{d}{L\omega}, \quad D_{\mu\mu} = D\left(\frac{\mathrm{v}}{\mathrm{v}_{ph}}\right)^2.$$

Strength of electric field
(RF power)

Magnetic field gradient
(B_{min} effect)

$V_{ph} \propto n_{cr}$

Higher critical density
(higher frequency)
Higher phase velocity

Smaller diffusion coefficient of pitch angle

A. Girard et al, J. Computational Phys. 191(2003)228

Frequency effect (theoretical calculation)

Fokker -Planck equation

Collision term | HF term | Source term

$$\frac{\partial f_e}{\partial t} = C(f_e)+Q(f_e)+S(f_e)$$

$$Q=\frac{1}{v^2}\frac{\partial}{\partial v}\left(v^2 D_{vv}\frac{\partial f_e}{\partial v}\right)+\frac{1}{v^2}\frac{\partial}{\partial \mu}\left((1-\mu^2)D_{\mu\mu}\frac{\partial f_e}{\partial \mu}\right)$$

$$D_{vv}=D=\frac{4}{3}\pi\left(\frac{eE}{2m_e}\right)^2\frac{d}{L\omega},\qquad D_{\mu\mu}=D\left(\frac{v}{v_{ph}}\right)^2.$$

Strength of electric field
(RF power)

Magnetic field gradient
(B_{min} effect)

$V_{ph} \propto n_{cr}$

Higher critical density
(higher frequency)
Higher phase velocity

Smaller diffusion coefficient of pitch angle

Power absorption

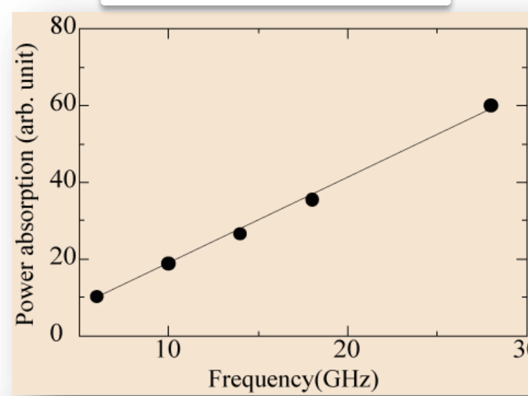

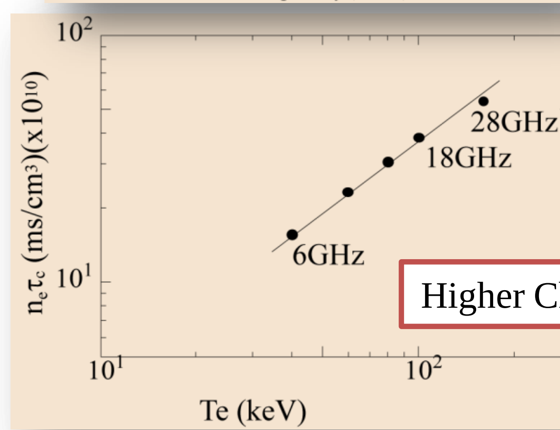

Higher Charge state

A. Girard et al, J. Computational Phys. 191(2003)228

High performance SC-ECRIS I –VENUS 28GHz-

Re-commissioning VENUS (18+28GHz)2010	
Xe^{26+}	480 eμA
Xe^{27+}	411 eμA
Xe^{30+}	211 eμA
Xe^{32+}	108 eμA
Xe^{35+}	38 eμA

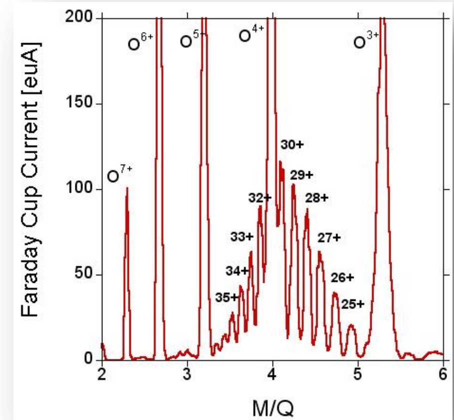

D. Leitner , et al, Proc. Int. Workshop on ECR ion sources, 2010, Grenoble, France,p11

Tuning Parameters	
28 +18 Ghz	5-6 kW
Bmin	.56 T
Bmin 18 GHz	87.5%
Bmin 28 GHz	56 %
Heat load into the cryostat	1.7 W

VENUS was the first high magnetic field SC-ECR ion source developed for operating at 28 GHz. A number of modifications were carried out during its development, for example, the special cramping technique of the hexapole magnet to increase the radial magnetic field. The modifications of the VENUS were then incorporated into the design of new SC-ECR ion sources.

High performance SC-ECRIS I –VENUS 28GHz-

Re-commissioning VENUS (18+28GHz)2010	
Xe^{26+}	480 eμA
Xe^{27+}	411 eμA
Xe^{30+}	211 eμA
Xe^{32+}	108 eμA
Xe^{35+}	38 eμA

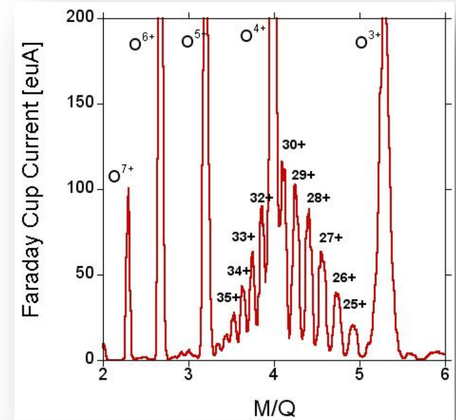

U^{33+} ~440eμA @8kW(18+28GHz)

(required beam intensity-FRIB,RISP)

D. Leitner , et al, Proc. Int. Workshop on ECR ion sources, 2010, Grenoble, France,p11

Tuning Parameters	
28 +18 Ghz	5-6 kW
Bmin	.56 T
Bmin 18 GHz	87.5%
Bmin 28 GHz	56 %
Heat load into the cryostat	1.7 W

VENUS was the first high magnetic field SC-ECR ion source developed for operating at 28 GHz. A number of modifications were carried out during its development, for example, the special cramping technique of the hexapole magnet to increase the radial magnetic field. The modifications of the VENUS were then incorporated into the design of new SC-ECR ion sources.

High performance SC-ECRIS II -SECRAL 24GHz-

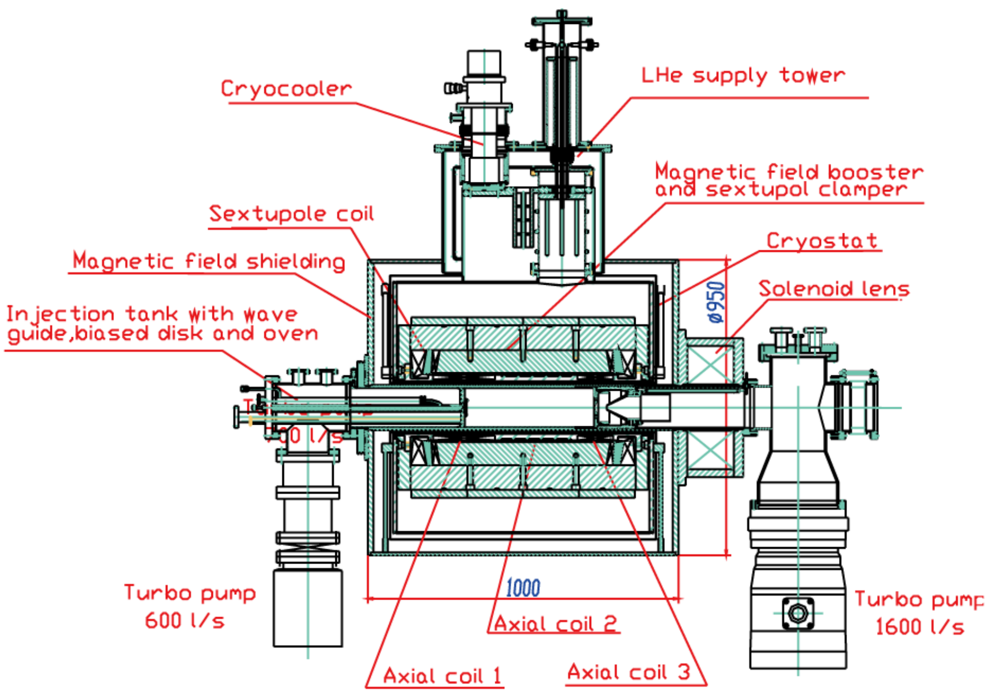

H. W. Zhao et al, Proc. Int. Workshop on ECR ion sources, 2010, Grenoble, France,p1

SECRAL (18(+14.5)GHz) RF power (kW) <3.2		SECRAL (24GHz) RF power (kW) 3~5	
$^{129}Xe^{20+}$	505eμA		
$^{129}Xe^{27+}$	306 eμA	$^{129}Xe^{27+}$	455 eμA
$^{129}Xe^{30+}$	101 eμA	$^{129}Xe^{30+}$	152 eμA
$^{129}Xe^{31+}$	68 eμA	$^{129}Xe^{31+}$	85 eμA
$^{129}Xe^{35+}$	16 eμA	$^{129}Xe^{35+}$	60 eμA
$^{129}Xe^{38+}$	6.6 eμA	$^{129}Xe^{38+}$	17 eμA
$^{129}Xe^{42+}$	1.5 eμA	$^{129}Xe^{42+}$	3 eμA
$^{129}Xe^{43+}$	1 eμA		

SECRAL is a compact SC-ECR ion source designed to operate at microwave frequencies of 18–28 GHz. The unique feature of the SECRAL source is its unconventional magnetic structure, in which superconducting solenoid coils are placed inside the superconducting sextupole. One of the advantages of this structure is that the magnet assembly can be compact in size as compared to similar high magnetic field ECR sources with conventional magnetic structures.

High performance SC-ECRIS II -SECRAL 24GHz-

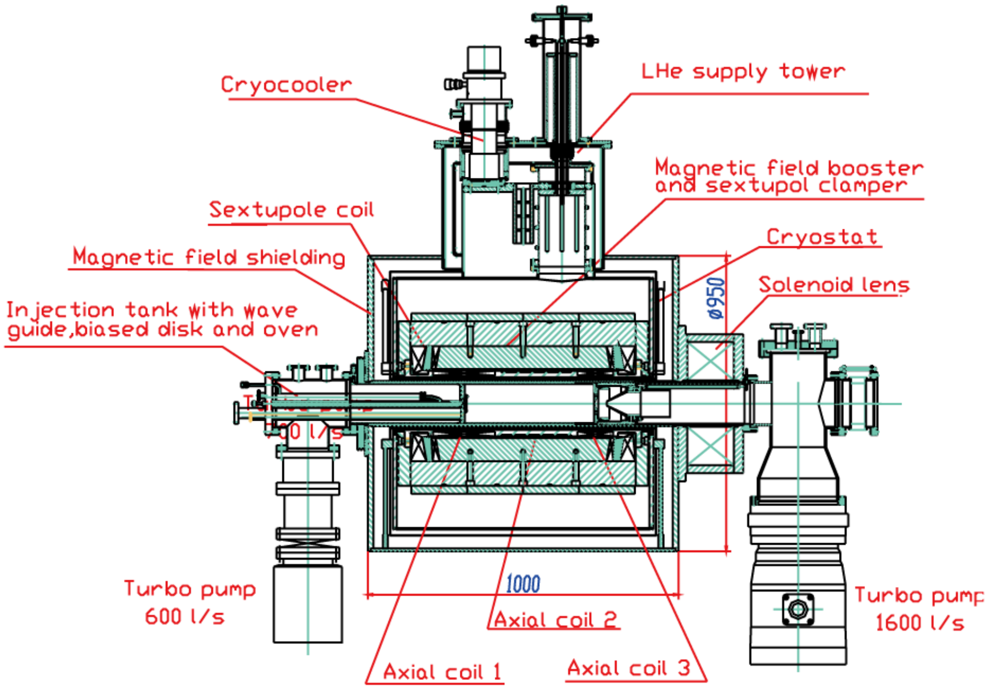

H. W. Zhao et al, Proc. Int. Workshop on ECR ion sources, 2010, Grenoble, France,p1

SECRAL (18(+14.5)GHz) RF power (kW) <3.2		SECRAL (24GHz) RF power (kW) 3~5	
$^{129}Xe^{20+}$	505eμA		
$^{129}Xe^{27+}$	306 eμA	$^{129}Xe^{27+}$	455 eμA
$^{129}Xe^{30+}$	101 eμA	$^{129}Xe^{30+}$	152 eμA
$^{129}Xe^{31+}$	68 eμA	$^{129}Xe^{31+}$	85 eμA
$^{129}Xe^{35+}$	16 eμA	$^{129}Xe^{35+}$	60 eμA
$^{129}Xe^{38+}$	6.6 eμA	$^{129}Xe^{38+}$	17 eμA
$^{129}Xe^{42+}$	1.5 eμA	$^{129}Xe^{42+}$	3 eμA
$^{129}Xe^{43+}$	1 eμA		

Bi^{36+} beam

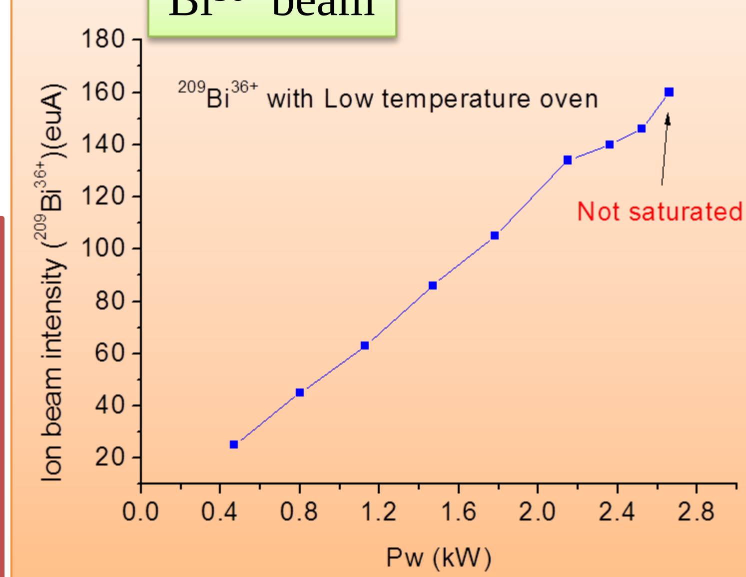

SECRAL is a compact SC-ECR ion source designed to operate at microwave frequencies of 18−28 GHz. The unique feature of the SECRAL source is its unconventional magnetic structure, in which superconducting solenoid coils are placed inside the superconducting sextupole. One of the advantages of this structure is that the magnet assembly can be compact in size as compared to similar high magnetic field ECR sources with conventional magnetic structures.

High performance SC-ECRIS III- RIKEN 28GHz-

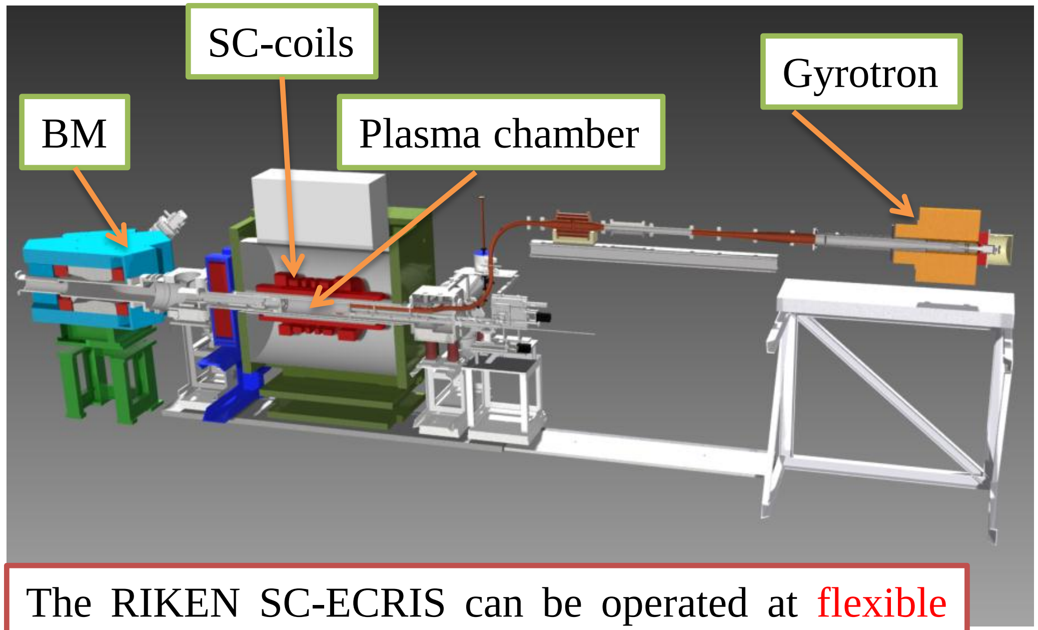

The RIKEN SC-ECRIS can be operated at flexible axial field distributions with six solenoid coils

It is possible to change the gradient of the magnetic field strength and the surface size of the ECR zone.

The RIKEN 28GHz SC ECRIS produced ~180eμA of U^{35+}, ~225 eμA of U^{33+} with the sputtering method at the injected RF power of ~4kW (28GHz).

T. Nakagawa et al, Rev. Sci. Instrum.81 (2010) 02A320.

"Flat B_{min}" G. D. Alton and D. N. Smithe, Rev. Sci. Instrum. 65 (1994)775

High performance SC-ECRIS III- RIKEN 28GHz-

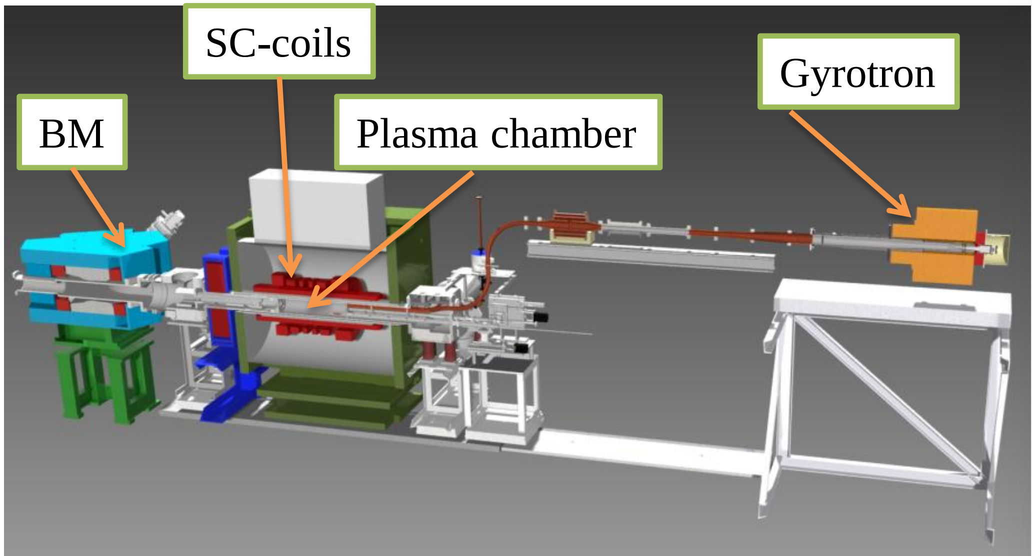

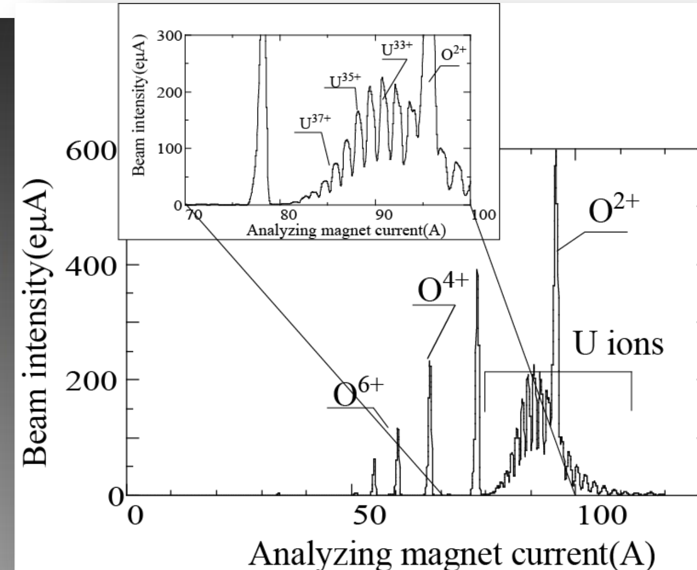

The RIKEN SC-ECRIS can be operated at flexible axial field distributions with six solenoid coils

It is possible to change the gradient of the magnetic field strength and the surface size of the ECR zone.

The RIKEN 28GHz SC ECRIS produced ~180eμA of U^{35+}, ~225 eμA of U^{33+} with the sputtering method at the injected RF power of ~4kW (28GHz).

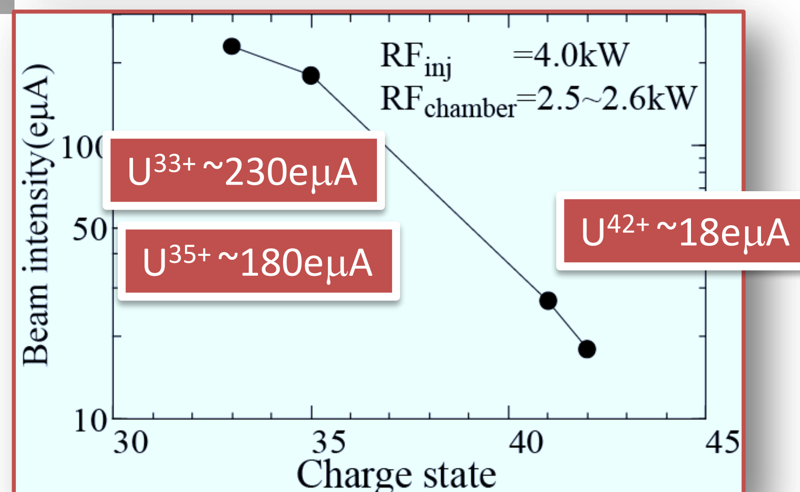

T. Nakagawa et al, Rev. Sci. Instrum.81 (2010) 02A320.

"Flat B_{min}" G. D. Alton and D. N. Smithe, Rev. Sci. Instrum. 65 (1994)775

Emittance

Magnetic field effect

$$\varepsilon_{magnet}^{xx'-norm} = 0.032 B_o \frac{q}{M}$$

Bo : axial magnetic field
q: charge state
M: mass

Cal: same q/M	same emittance
: higher Bo	larger emittance

Bo 18GHz ~1.2T
28GHz ~1.8T

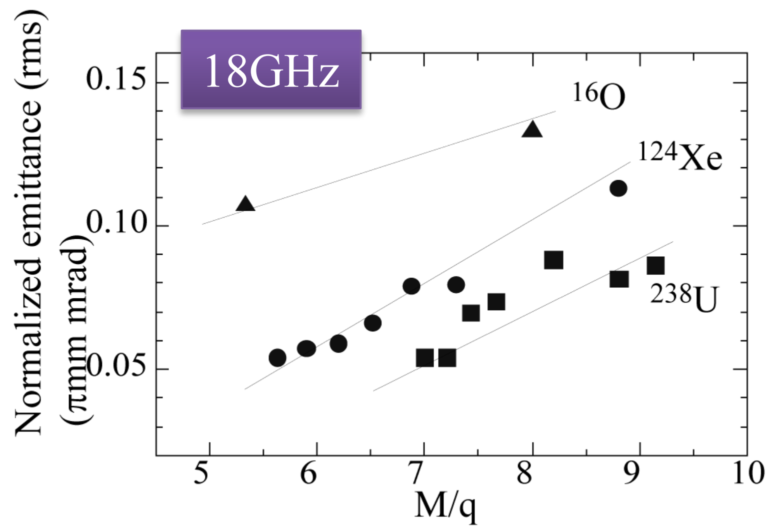

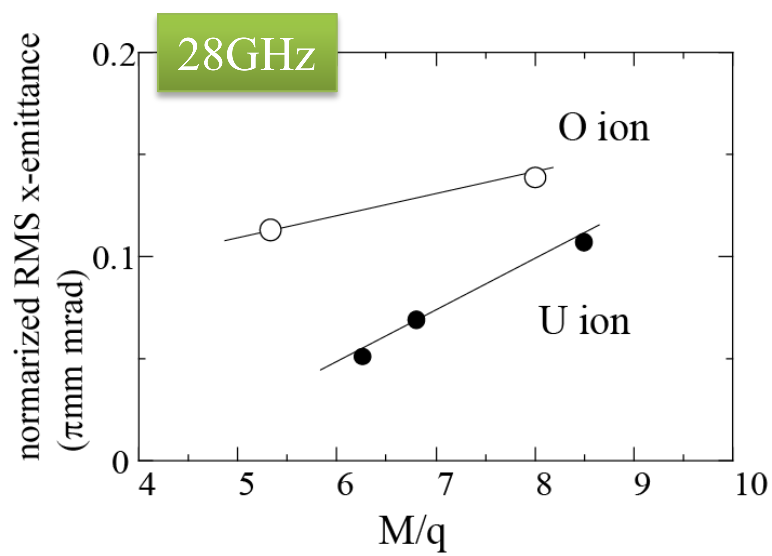

Emittance

Magnetic field effect

$$\varepsilon_{magnet}^{xx'-norm} = 0.032 B_o \frac{q}{M}$$

Bo : axial magnetic field
q: charge state
M: mass

Cal: same q/M	same emittance
: higher Bo	larger emittance

Bo 18GHz ~1.2T
28GHz ~1.8T

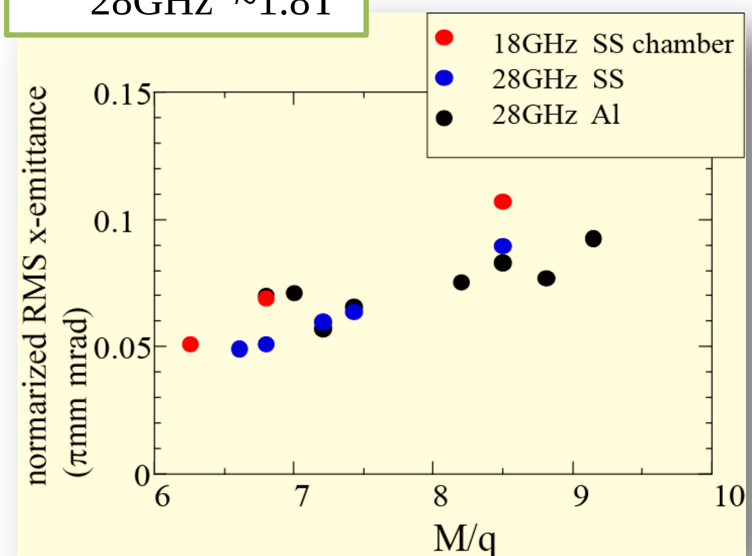

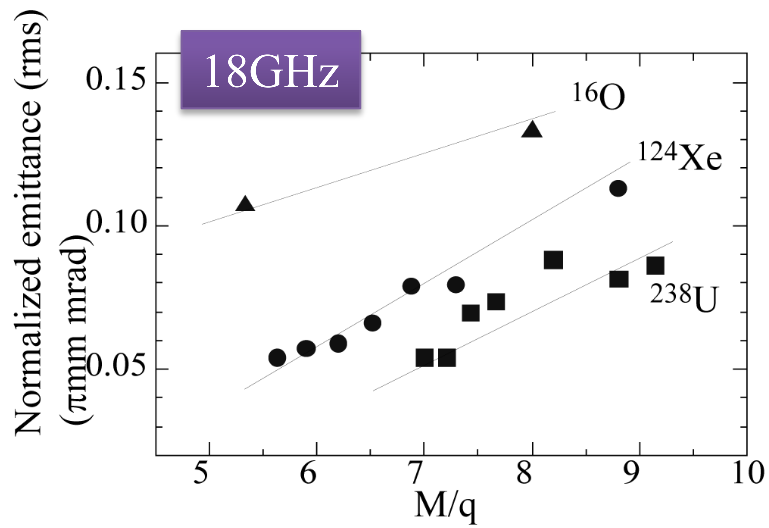

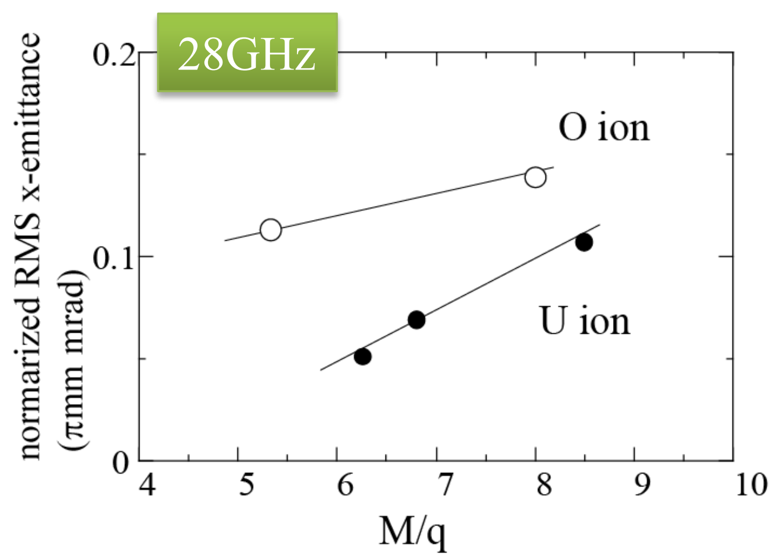

Limitation of the beam intensity increase I

RF power vs. gas pressure
(Fokker-Planck eq.)

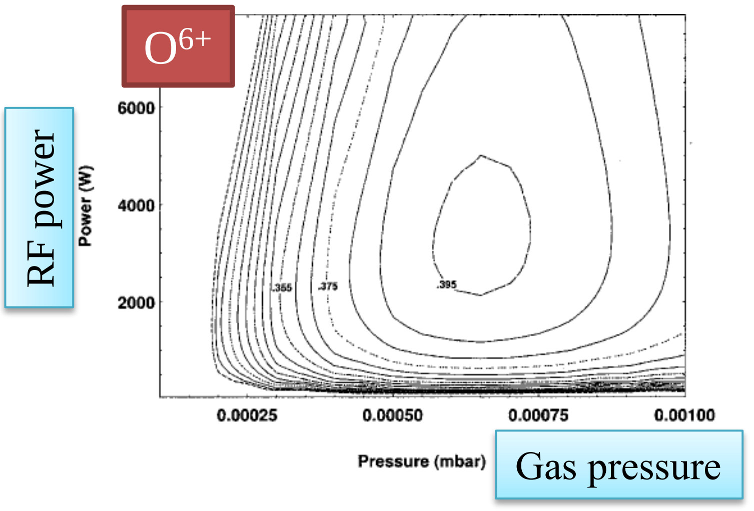

B. Cluggish et al, NIM A 631(2011)111

Limitation of the beam intensity increase I

RF power vs. gas pressure
(Fokker-Planck eq.)

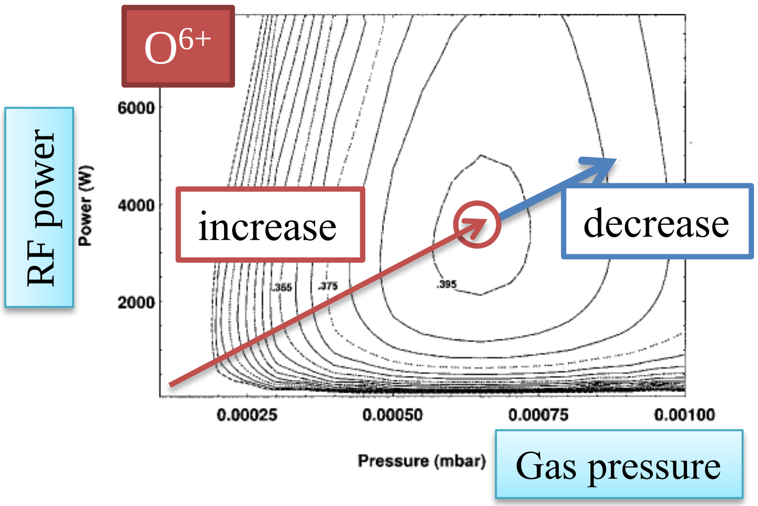

B. Cluggish et al, NIM A 631(2011)111

Limitation of the beam intensity increase I

RF power vs. gas pressure (Fokker-Planck eq.)

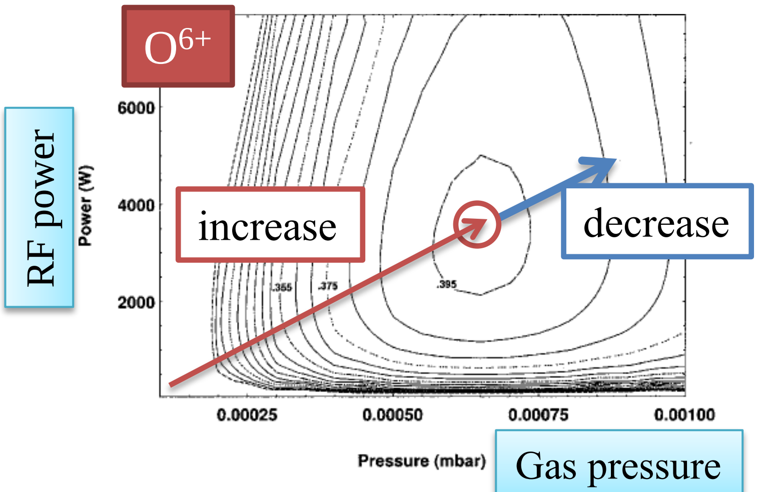

The effect of RF power on the plasma parameters (electron density, temperature and current) and high RF-power instability were demonstrated using FAR-TECH's generalized ECRIS model (GEM)].

These showed that the threshold of the RF power for the instability increased with an increase in the gas pressure. The origin of the instability was the pitch-angle scattering of the electrons by the ECR heating process.

FAR-TECH's Generalized ECRIS Model (GEM)

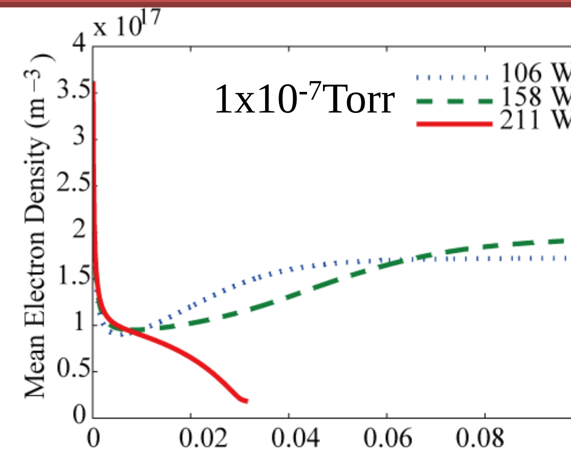

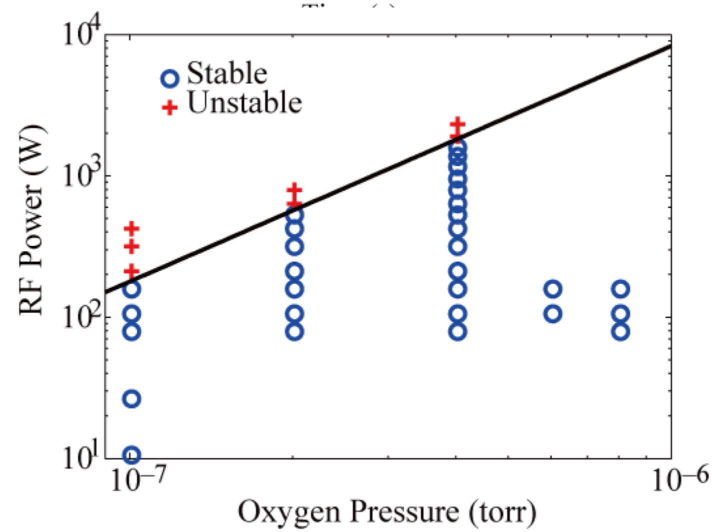

B. Cluggish et al, NIM A 631(2011)111

Experimental results (RF power dependence)

CAPRICE 14GHz

D. Hitz et al, RSI 71(2000)839

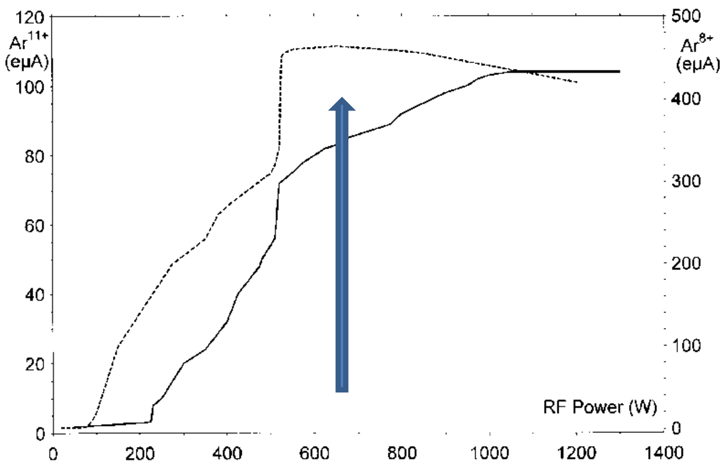

CAPRICE ~0.5L

Limitation >1~2kW/L

Experimental results (RF power dependence)

CAPRICE 14GHz

D. Hitz et al, RSI 71(2000)839

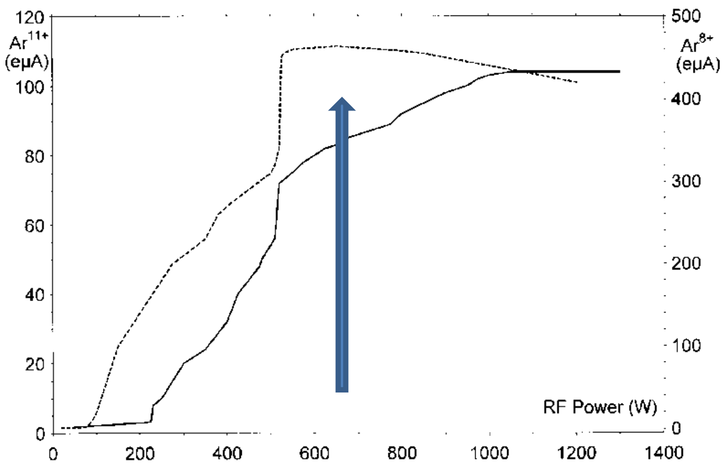

VENUS 28GHz

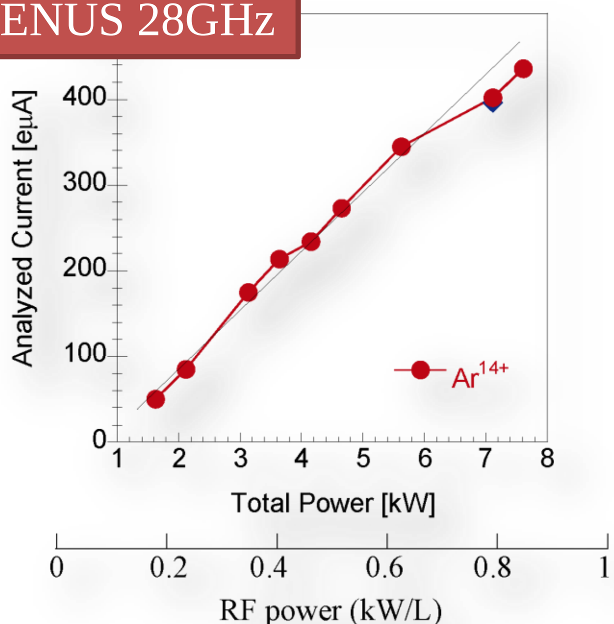

CAPRICE ~0.5L

Limitation >1~2kW/L

D. Leitner et al, HEP&NP 31(2007)1

Despite this important information, we have few experimental results for beam intensity saturation at present.

The beam intensity of high-performance SC-ECR ion sources that have a larger plasma chamber volume increases linearly and is not saturated at high power.

To clarify this phenomenon, we need to carry out further investigation under various conditions.

Effect of magnetic field

$$W_{power} = \left(\frac{\pi n e^2 E^2}{m\omega \left(\frac{dB}{dZ} \right)} \right) S_{ecr}$$

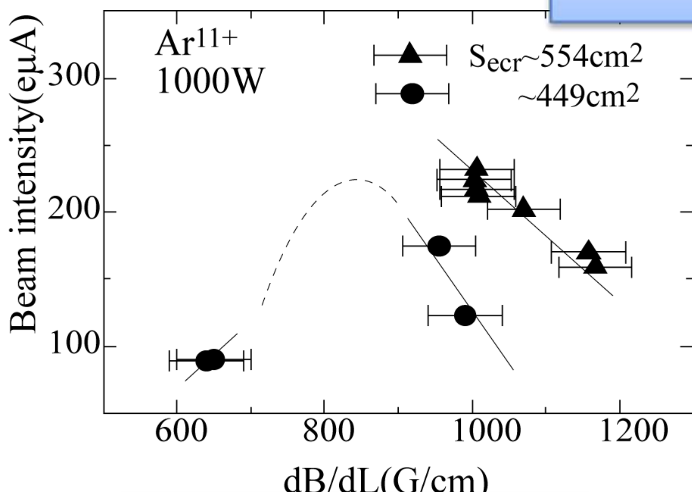

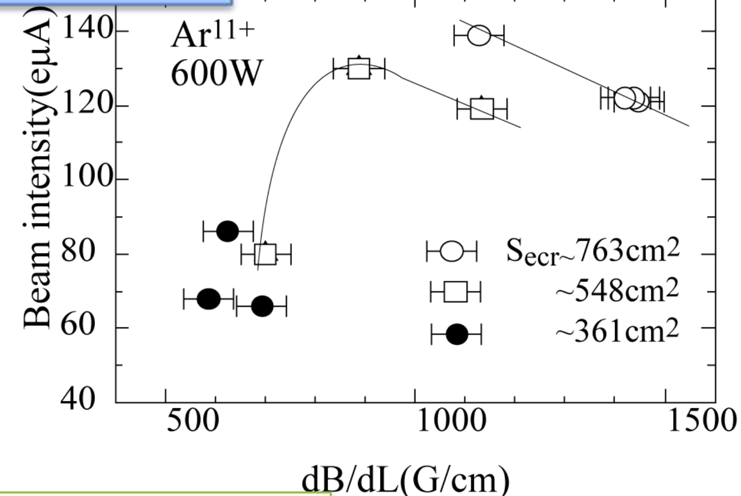

dB/dL~700~800G/cm
S_{ecr}<500cm^2

RF power ~1000~600W

Beam intensity decreases with decreasing the magnetic field gradient
Beam intensity becomes unstable
To clarify this phenomenon, we need to carry out further investigation under various conditions

Beam instability

Spectrum analyzer

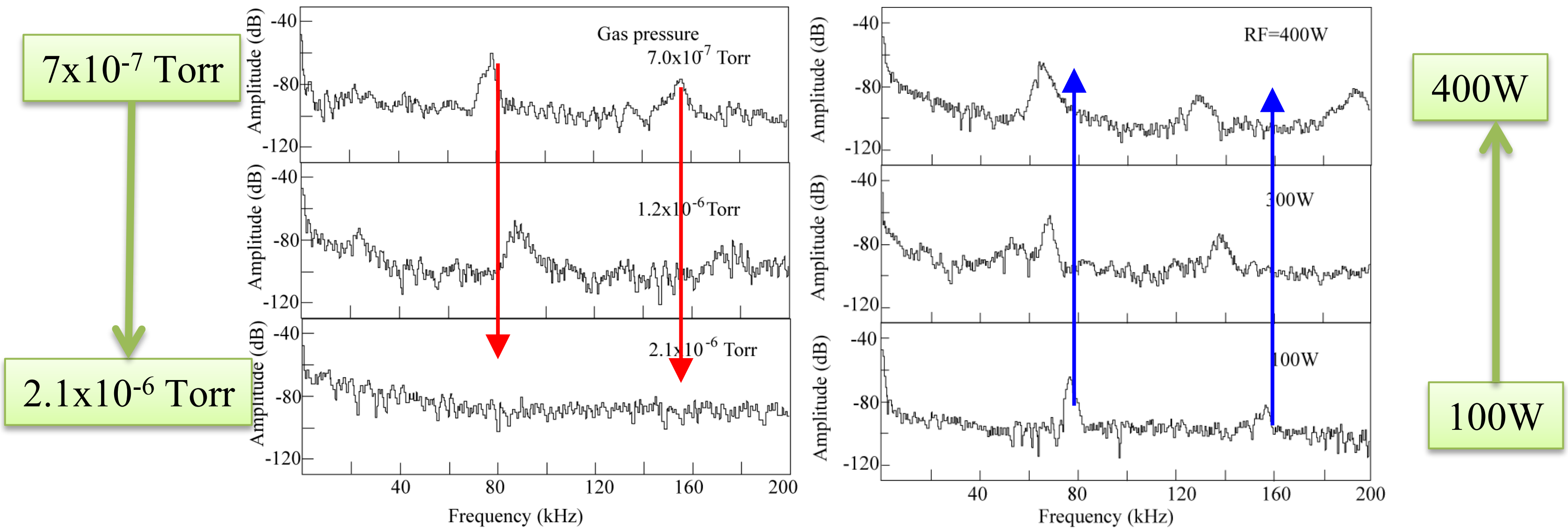

Gas pressure

Microwave Power

The beam intensity was strongly oscillated regularly.
The frequency was several 10 kHz~few 100kHz
The peaks were shifted by changing the RF power and gas pressure.
The amplitude increases with decreasing the gas pressure or increasing the RF power (plasma instabilities?)
Beam stability is very important factor for accelerator

36GHz ECRIS

Required magnetic field strength

B_{inj}	~ 5T
B_r	~2.7T
B_{ext}	~2.7T
B_{min}	0.8~1.2T

Example of RIKEN 28GHz ECRIS

28GHz → 36GHz

36GHz ECRIS

Required magnetic field strength

B_{inj}	~ 5T
B_r	~2.7T
B_{ext}	~2.7T
B_{min}	0.8~1.2T

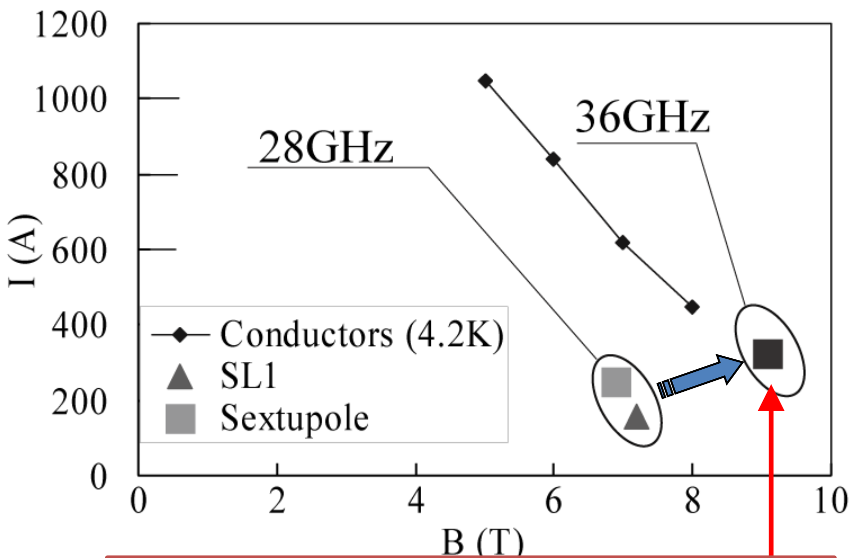

Example of RIKEN 28GHz ECRIS

28GHz → 36GHz

Exceed the critical current of NbTi wire at 4.2K

Solution

1) Use of NbTi wire at low temperature (<4.2K)
2) Use of other super-conducting wires (Nb_3Sn)
3)New structure SC-ECRIS

36GHz ECRIS

Required magnetic field strength

B_{inj}	~ 5T
B_r	~2.7T
B_{ext}	~2.7T
B_{min}	0.8~1.2T

Example of RIKEN 28GHz ECRIS

28GHz ⇒ 36GHz

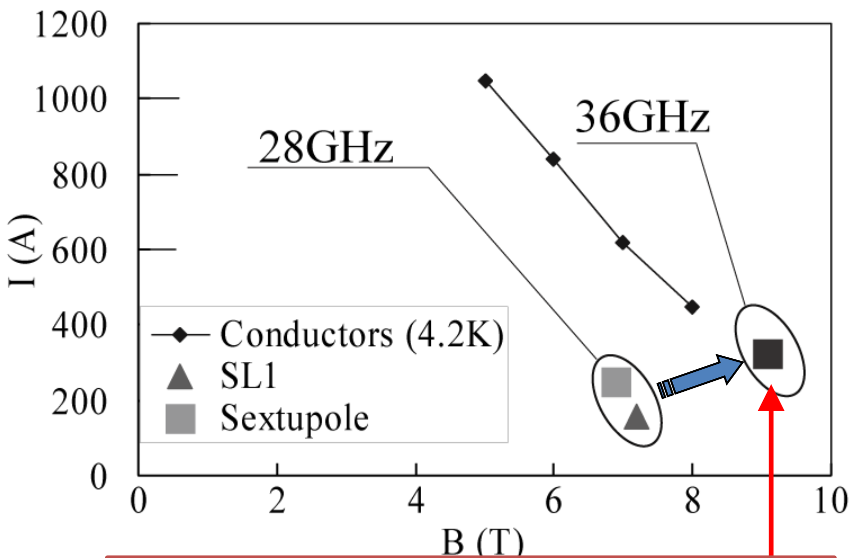

Exceed the critical current of NbTi wire at 4.2K

Solution

1) Use of NbTi wire at low temperature (<4.2K)
2) Use of other super-conducting wires (Nb_3Sn)
3)New structure SC-ECRIS

Z.Q. Xie, Rev. Sci. Instrum. 83 (2012) 02A302.
C. Lyneis et al, Rev. Sci. Instrum. 83 (2012) 2A301.

X-ray heat load

To produce intense highly charged heavy ions, we need higher B_{min} and lower gas pressure

In this case, heat load of X-ray becomes very high as shown in these figures

Ex. B_{min}~$0.8B_{ecr}$ RF power~6kW
We will obtain 6W of X-ray heat load

Solutions
1)Use of large refrigerator (GM-JT) to obtain higher cooling power (~10W)
2)To find new method to minimizing the X-ray heat load while keeping the beam intensity

RF power effect

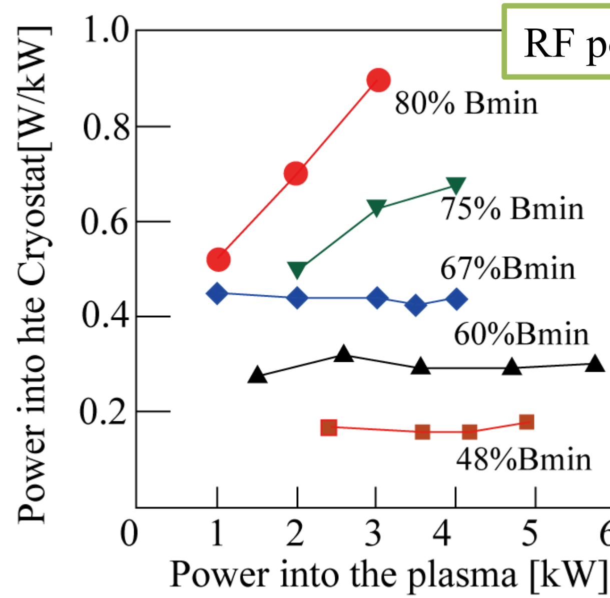

D. Leitner , et al, Proc. Int. Workshop on ECR ion sources, 2010, Grenoble, France,p11

Gas pressure effect

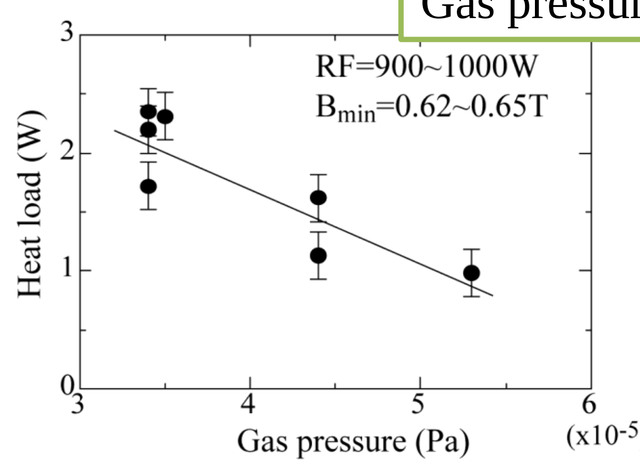

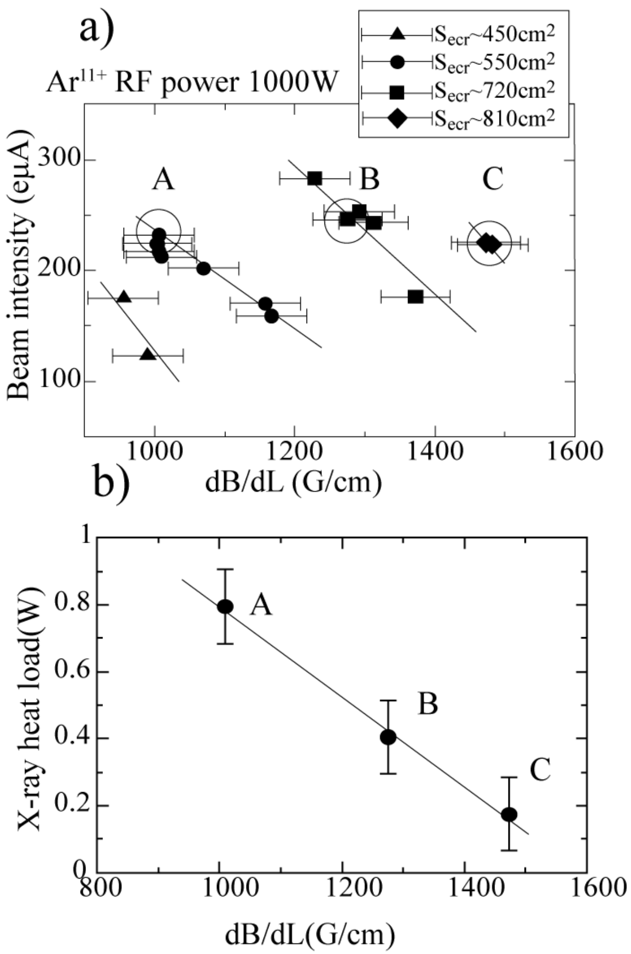

Lager zone size and steeper field gradient gives lower X-ray heat load

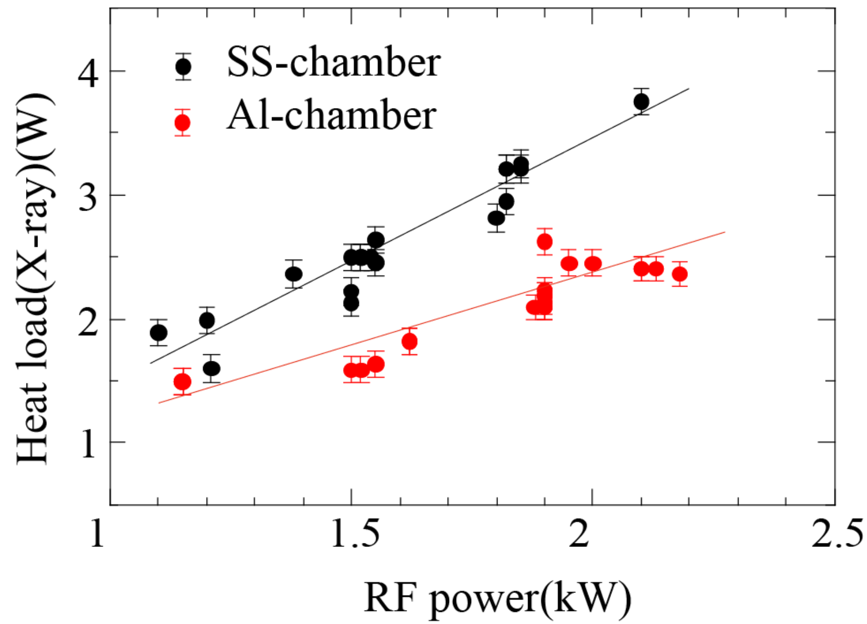

X-ray heat load using Al-chamber is lower than that using SS-chamber